EAAGN17

4 - 6 December 2017 in Kagoshima, Japan

Spectral Energy Distributions of Fermi Blazars

费米耀变体的能谱分布

Junhui Fan 樊军辉

Guangzhou University 广州大学

Co-authors: JH Yang, Y Liu, Y.H. Yuan, J.M. Hao

C. Lin, H.B. Xiao, Z.Y. Pei, D Costantin

广州大学
Guangzhou University

Contents of the Talk

1. A brief introduction to blazars:
    - BL Lac + FSRQs
    - Classifications of BL Lacs
        - Surveys
        - Synchrotron Peak Frequency
            - Including our own work on the class.
                (Fan et al. 2016, ApJS, 226)
2. Some correlations
3. Beaming Effect
4. Summary

Outline

1. Introduction
2. Spectral Energy Distributions
3. Beaming Effect in Fermi Blazars
4. Summary

广州大学 Guangzhou University

Outline

1. Introduction
2. Spectral Energy Distributions
3. Beaming Effect in Fermi Blazars
4. Summary

Objects with one of the above properties → **BLAZARS**

BLAZARS (BL Lacs and FSRQs)

Special subclass of AGNs:

extragalactic objects with rapid variability, high luminosity, high and variable polarization, have/no strong emission lines, gamma-ray emissions, or superluminal motions.

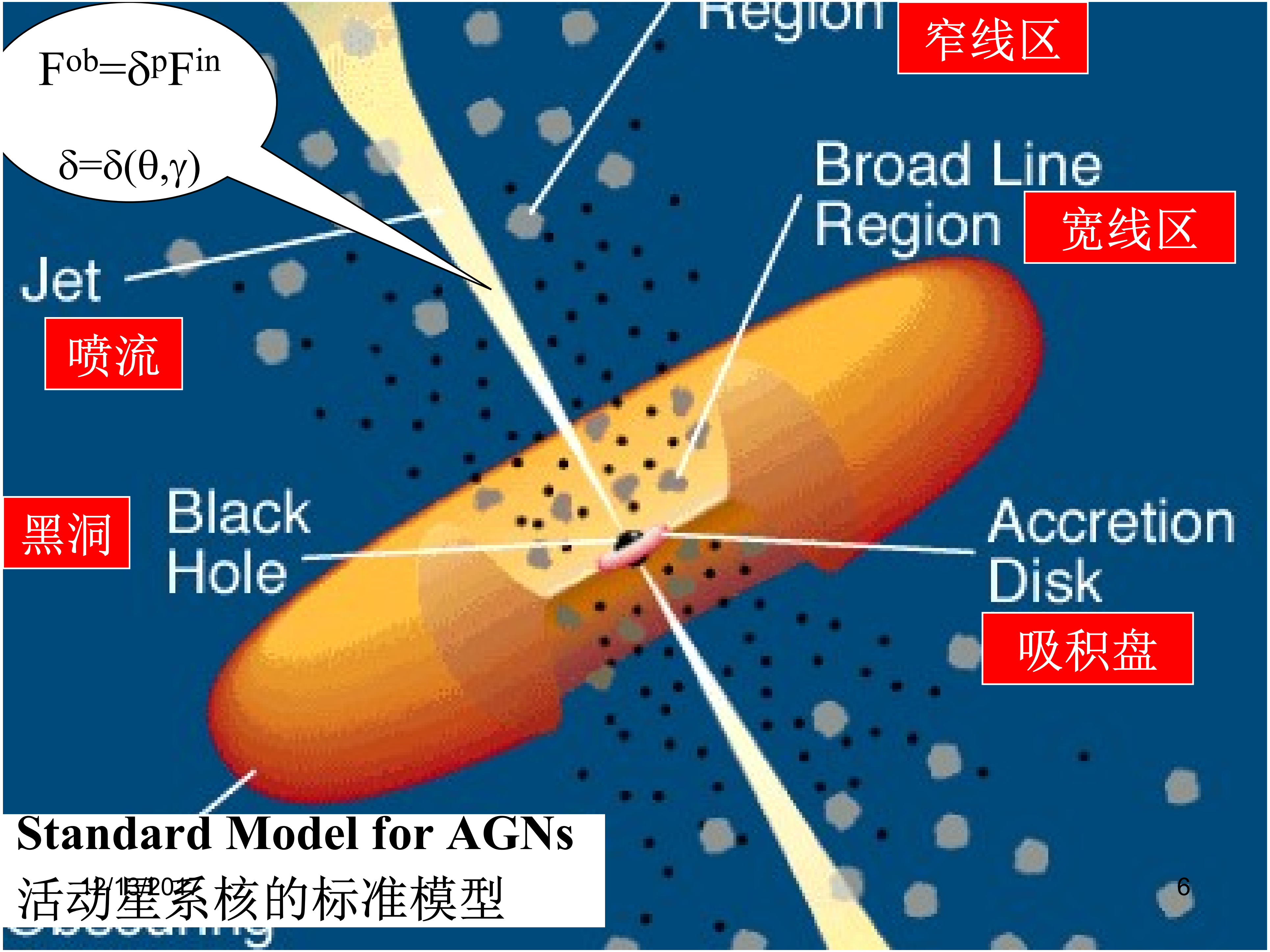

Standard Model for AGNs

活动星系核的标准模型

INTRODUCTION

1) BL Lacertae objects--BLs,

2) Flat Spectrum Radio Quasars—FSRQs

INTRODUCTION

BL Lacertae objects--BLs, { RBLs / XBLs }

- RBLs
- XBLs

这种分类不是基于物理的

Classification of BL Lac Objects

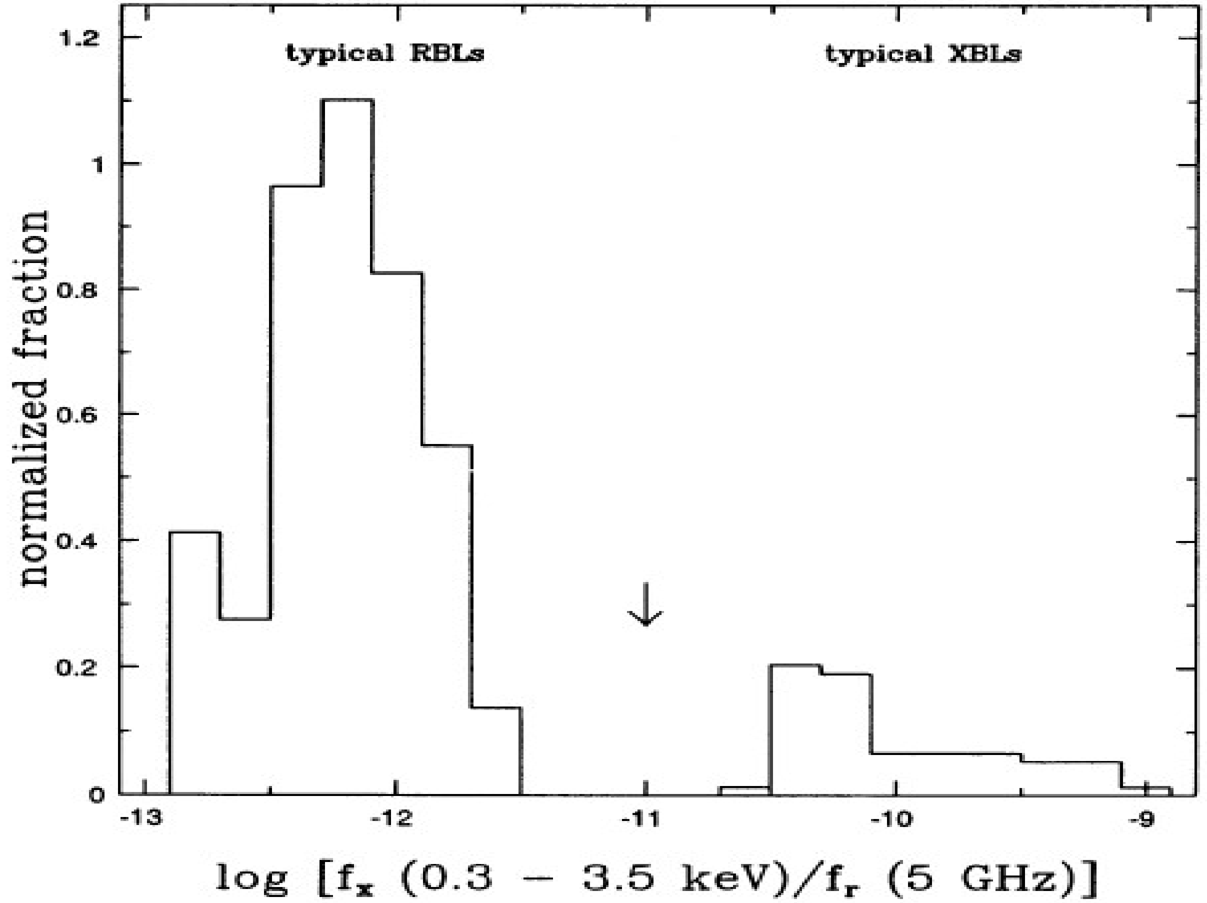

FIG. 2.—Assumed distribution of ratios of X-ray to radio flux for the whole L Lac population (see text for details). The arrow indicates the dividing line etween RBL-like and XBL-like objects. X-ray fluxes cover the 0.3–3.5 keV nge and are in units of ergs cm^{-2} s^{-1}, while radio fluxes refer to 5 GHz and e expressed in janskys.

基于物理的分类

Padovani & Giommi 1995, ApJ, 444

Classification of BL Lac Objects

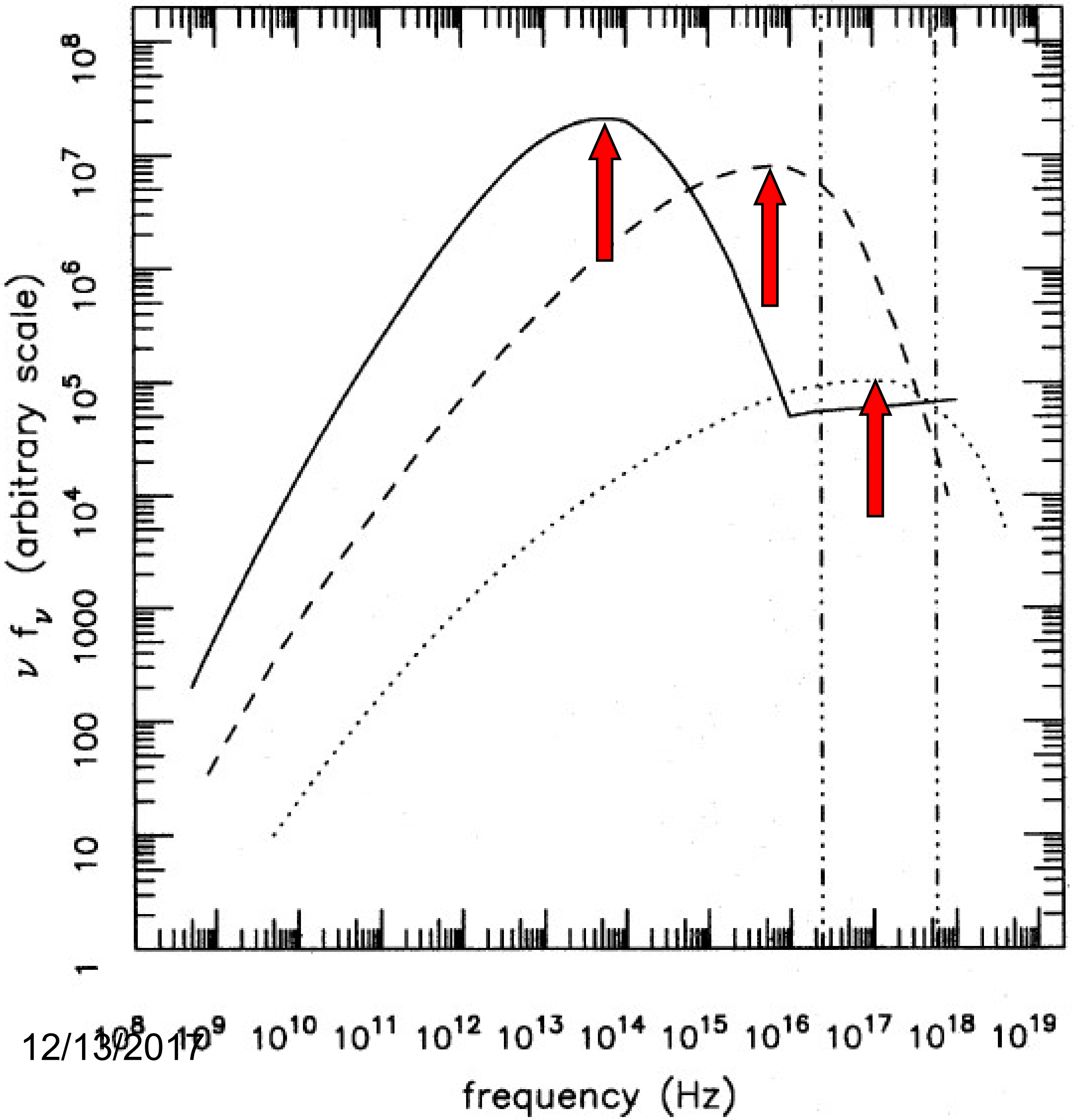

Padovani & Giommi 1996

Classification of BL Lac Objects

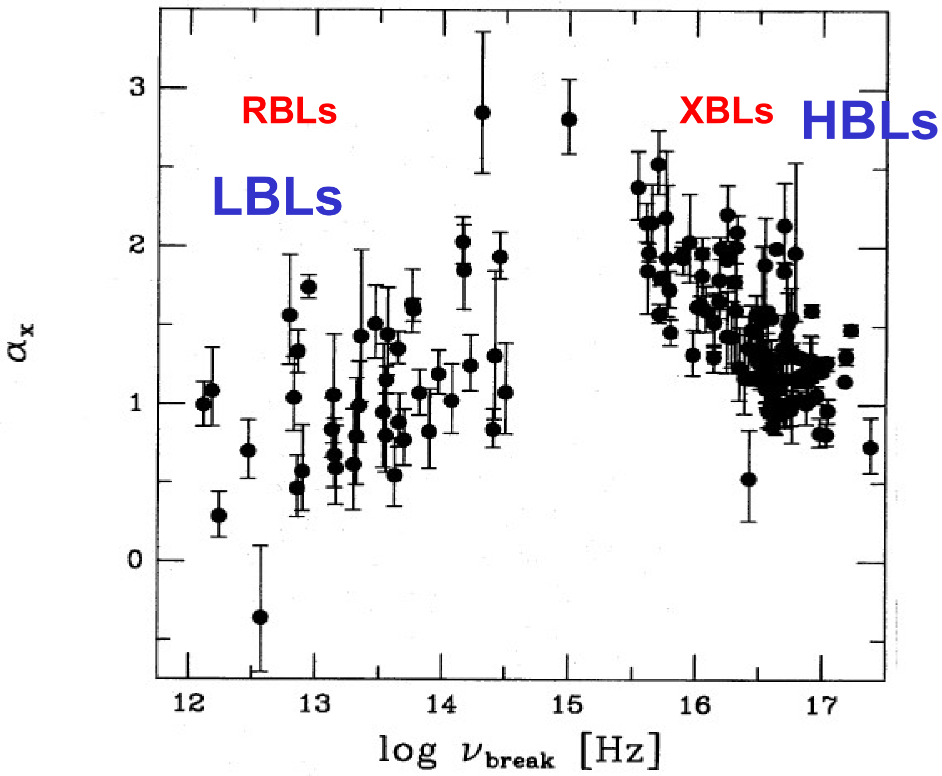

提出用峰频分类

LBLs:

Low-frequency peaked

HBLs:

High-frequency peaked

α_{ox}

XBL ⟷ HBL, RBL ⟷ LBL

Padovani & Giommi 1996

SED of Blazars
Fossati et al. 1998

Compiled 3 subclasses of 126 blazars (RBLs, XBLs, FSRQs)

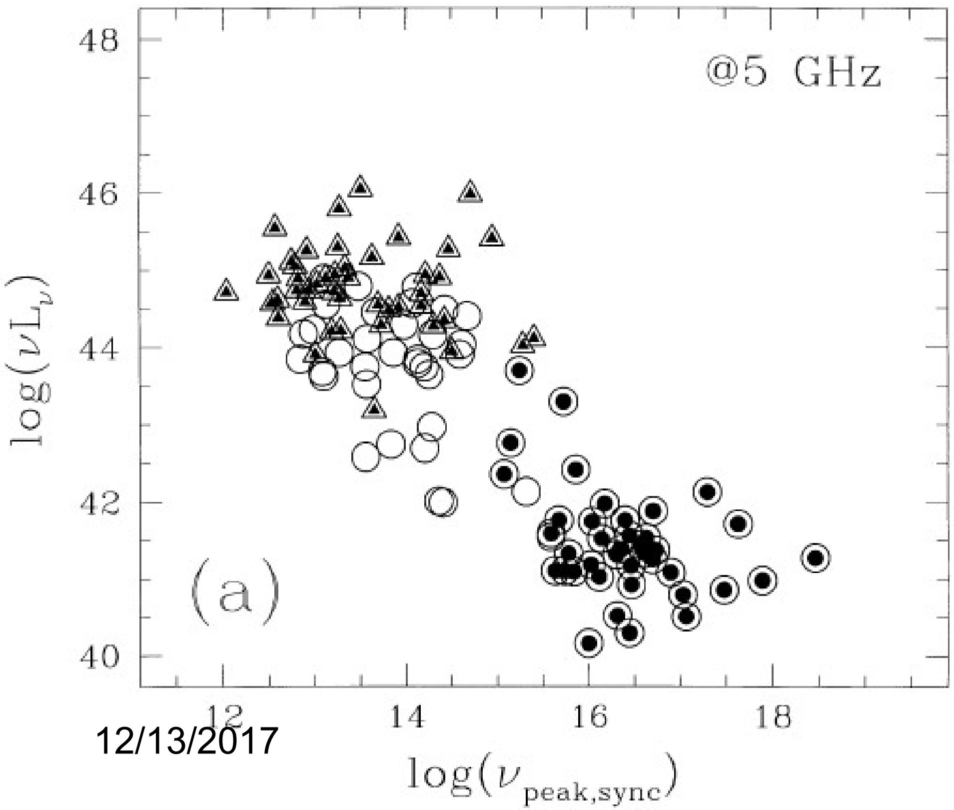

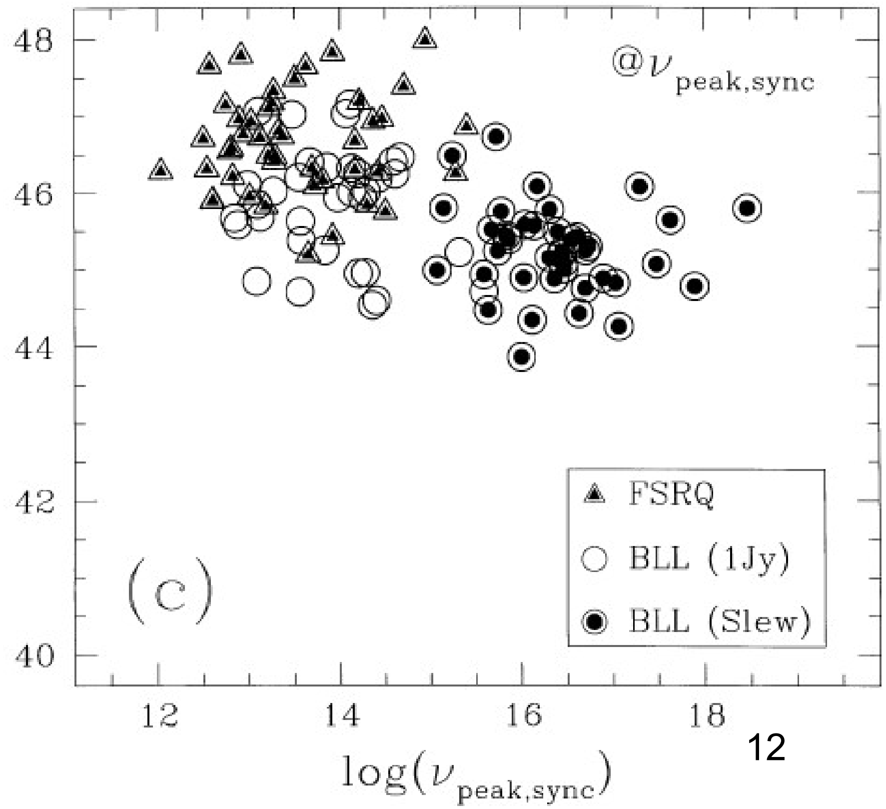

Sequence of Blazars

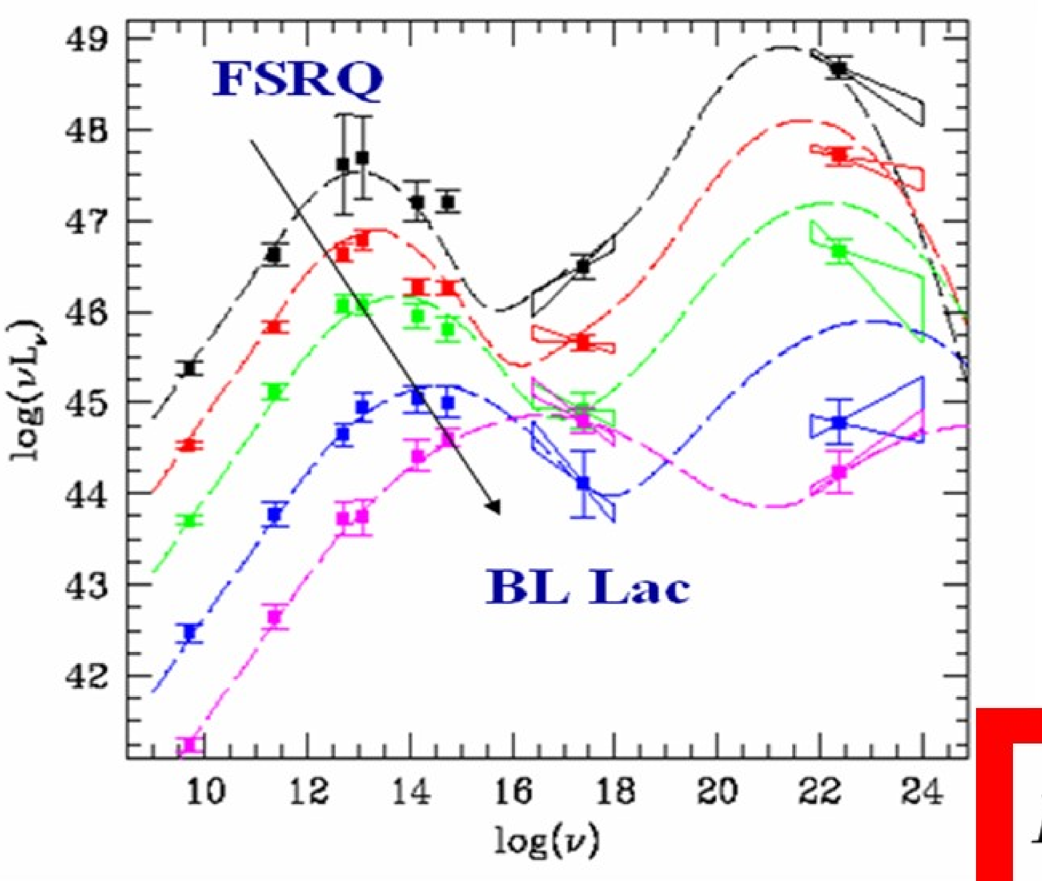

提出**Blazar**序列

$$FSRQs \rightarrow RBLs \rightarrow XBLs$$

$$\nu_p^{FSRQs} < \nu_p^{RBLs} < \nu_p^{XBLs}$$

$$L_{\nu_p}^{FSRQs} > L_{\nu_p}^{RBLs} > L_{\nu_p}^{XBLs}$$

Giommi et al. 2005, A&A, 434, 385

Detected luminous high frequency BL Lacs

low frequency low luminosity BL Lacs

Contradic ”

since t ; low
frequen ous BL Lacs
in Foss

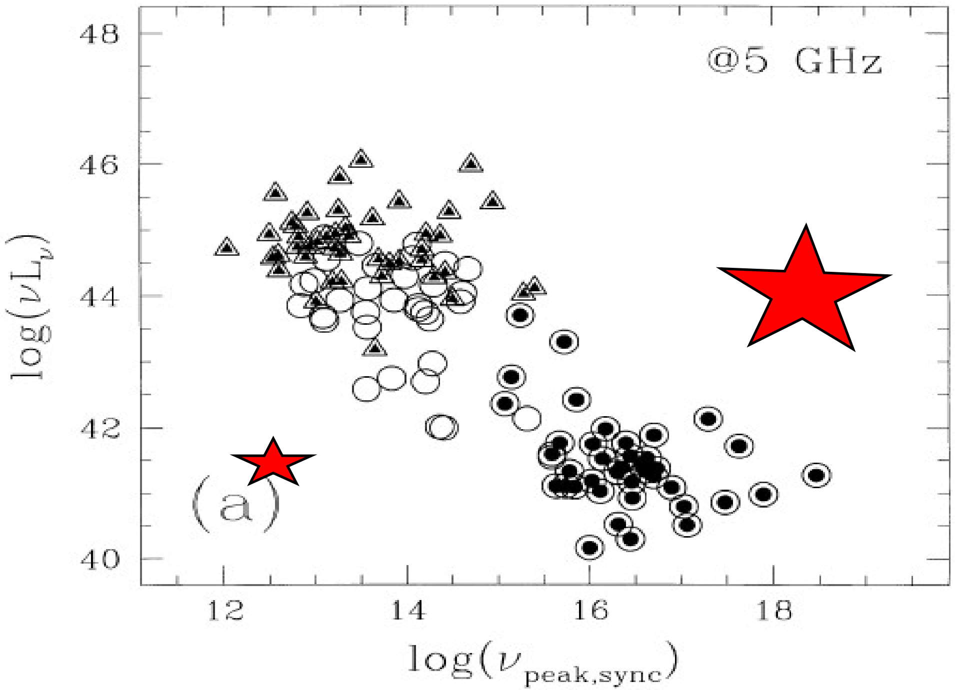

Niepploa et al. 2006, A&A, 445, 441

提出IBL

- Calculated SEDs for 308 blazars and set roughly frequency boundary for subclasses of BL Lacs (based on P & G criteria).

LBLs: $\log\nu_{\rm p} < 14.5$

IBLs: $14.5 < \log\nu_{\rm p} < 16.5$

HBLs: $\log\nu_{\rm p} > 16.5$

$$\nu_{syn}^{FSRQs} \rightarrow \nu_{syn}^{LBLs} \rightarrow \nu_{syn}^{IBLs} \rightarrow \nu_{syn}^{HBLs}$$

Fermi/LAT

- Launch from Cape Canaveral Air Station 11 June 2008 at 12:05PM EDT
- Circular orbit, 565 km altitude (96 min period), 25.6 deg inclination.

Abdo, et al. 2010, ApJ, 715, 429

set frequency boundary for subclasses of ~ 48 blazars (based on P & G criteria, according to their position in the effective spectral index plot).

LSPs: $\log\nu_{\rm p} < 14.$

ISPs: $14. < \log\nu_{\rm p} < 15$

HSPs: $\log\nu_{\rm p} > 15$

Lower, Intermediate, High Synchrotron Peak

提出不分**FSRQs**和**BL**天体

Boundaries for Classifications

LBL Log ν (Hz)	IBL Log ν (Hz)	HBL Log ν (Hz)	Ref
< 15		> 15	Padovani & Giommi, 1996
< 14.5	14.5 ~ 16.5	> 16.5	Nieppola et al. 2006
<14	14 ~ 15	> 15	Abdo et al. 2010

Non Consensus

UHSP BL Lacs

- Ghisellini (1999) proposed that there is a subclass of BL Lacs: HBLs, p > 10^{19} *Hz.*
- Giommi et al. (2001) : Ultra-high-energy synchrotron peak BL Lacs (UHBLs).
- Nieppola et al. (2006): there are 22 objects with log p > *19, of which* 9 objects have log p > *20.*

广州大学 Guangzhou University

Outline

1. Introduction
2. Spectral Energy Distributions
3. Beaming Effect in Fermi Blazars
4. Summary

2.1 SEDs for 1425 Fermi Blazars from 3FGL

Fan et al. 2016, ApJS, 226, 20

Fan et al 2016, ApJS, 226,20

Calculating the SEDs for 1425 Fermi blazars from 3FGL using their multiwavelength flux density by fitting

$$\log\nu F_\nu = P_1(\log\nu - P_2)^2 + P_3$$

SEDs are successfully obtained for 1392 sources.

To do correlation analysis

2.1 Fitting Results for some sources

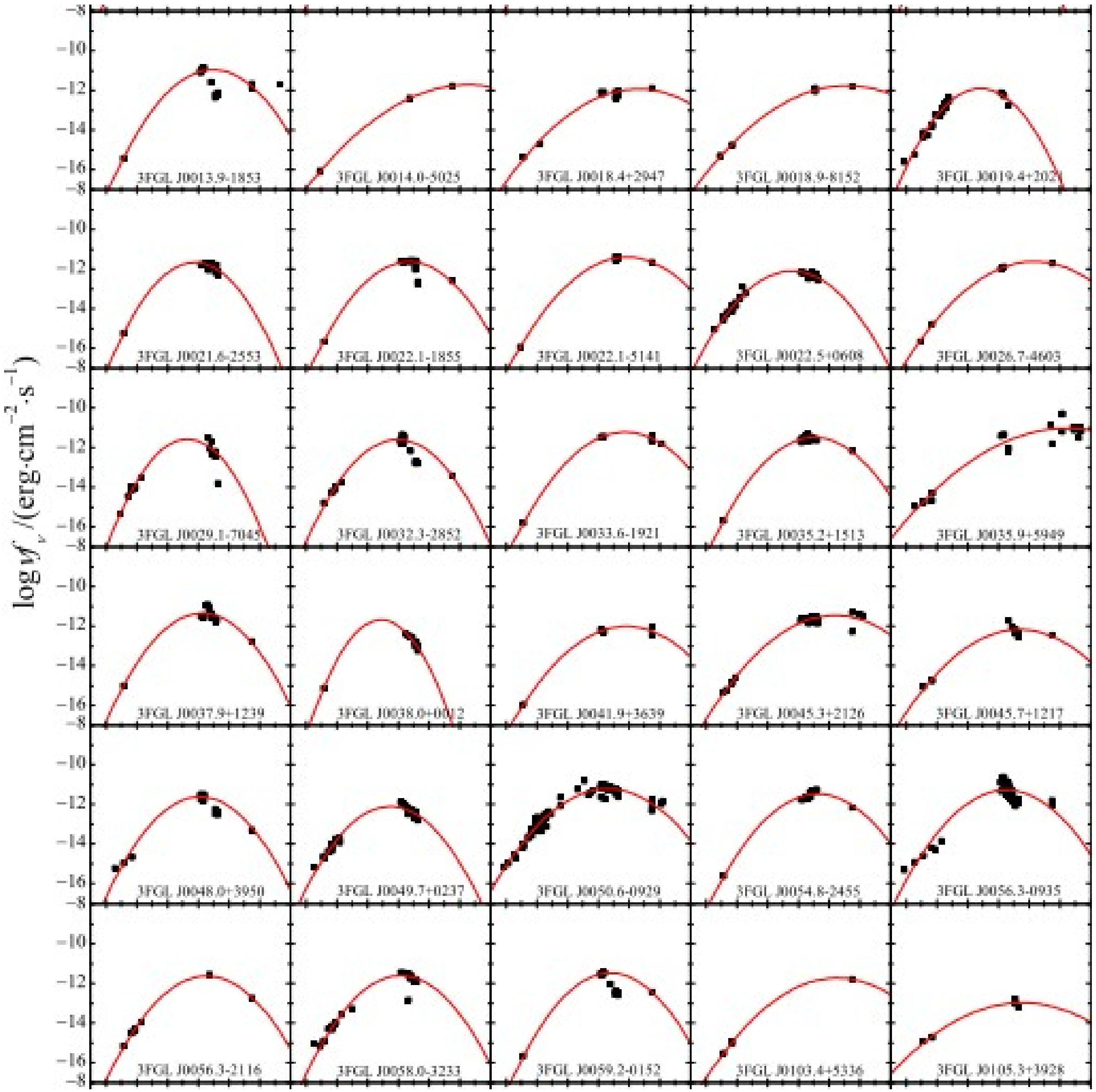

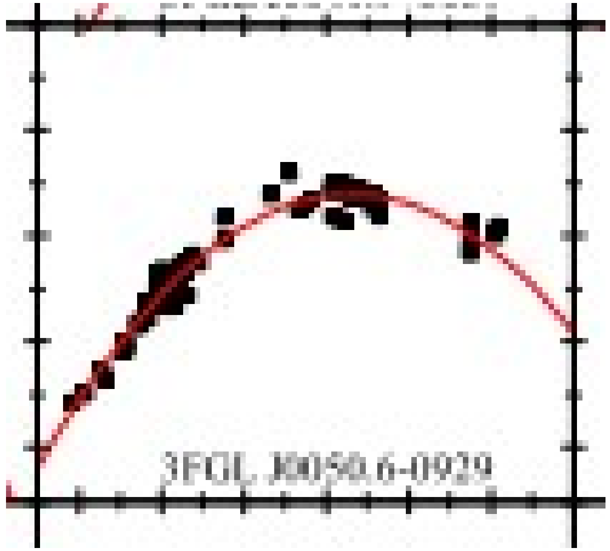

广州大学 Guangzhou University

Table 1. Sample for blazars

3FGL name	z	C	L_R/σ_{L_R}	L_O/σ_{L_O}	L_X/σ_{L_X}	$L_\gamma/\sigma_{L_\gamma}$	$\alpha_{RO}/\sigma_\alpha$	$\alpha_{OX}/\sigma_\alpha$	P_1/σ_{P_1}	ν_p/σ_{ν_p}	L_p/σ_{L_p}	$L_{bol}/\sigma_{L_{bol}}$
(1)	(2)	(3)	(4)	(5)	(6)	(7)	(8)	(9)	(10)	(11)	(12)	(13)
J0001.2-0748		IB	42.36/0.01	45.39/0.02		45.23/0.06	0.45/0.01		-0.12/0.01	14.37/0.12	45.35/0.03	45.71/0.05
J0001.4+2120	1.106	HF	42.97/0.01			45.73/0.11			-0.05/0.00	16.79/0.28	45.70/0.03	46.32/0.04
J0003.2-5246		HJ			45.13/0.07	44.30/0.11			-0.03/0.01	17.59/0.41	45.45/0.14	45.76/0.14
J0003.8-1151	1.310	LJ	43.44/0.01	45.54/0.04		45.59/0.12	0.62/0.01		-0.12/0.01	13.06/0.11	45.57/0.11	46.01/0.15
J0004.7-4740	0.880	IF		46.28/0.04	44.98/0.07	45.85/0.05		1.52/0.04	-0.12/0.01	14.14/0.09	46.20/0.06	46.59/0.09
J0006.4+3825	0.229	IF	41.98/0.01	44.53/0.04	43.44/0.07	44.41/0.06	0.54/0.01	1.40/0.04	-0.11/0.01	14.03/0.12	44.55/0.10	45.08/0.14
J0008.0+4713	0.280	IB	41.18/0.01		43.51/0.07	44.87/0.03			-0.12/0.00	14.52/0.07	44.46/0.04	44.83/0.06
J0008.6-2340	0.147	IB	40.36/0.01		43.72/0.05	43.05/0.12			-0.10/0.01	15.09/0.19	44.31/0.05	44.40/0.07
J0009.1+0630		LB	42.43/0.02	44.97/0.04		45.11/0.07	0.54/0.01		-0.09/0.03	13.69/0.51	44.12/0.17	44.93/0.24
J0009.6-3211	0.026	LJ	39.87/0.01	44.48/0.04	41.53/0.13	41.91/0.10	0.17/0.01	2.09/0.06	-0.16/0.02	13.93/0.21	43.30/0.17	44.11/0.23
J0013.2-3954		LB	42.74/0.02	45.04/0.04		45.21/0.05	0.58/0.01		-0.19/0.01	12.95/0.11	45.53/0.09	45.79/0.13
J0013.9-1853	0.095	IB	39.90/0.02		43.72/0.03	42.88/0.11			-0.13/0.01	14.96/0.15	44.37/0.07	44.65/0.09
J0014.0-5025		HB			45.05/0.07	44.64/0.10			-0.05/0.00	16.55/0.09	45.36/0.04	45.94/0.07
J0015.7+5552		HJ	41.90/0.01			44.93/0.09			-0.10/0.00	15.82/0.10	45.35/0.03	46.32/0.04
J0016.3-0013	1.577	IF	43.96/0.01	45.49/0.04	45.02/0.07	46.67/0.06	0.72/0.01	1.17/0.04	-0.09/0.01	13.58/0.13	45.58/0.04	46.12/0.06
J0017.2-0643		IU	41.94/0.01	44.82/0.04		44.87/0.09	0.48/0.01		-0.10/0.01	14.64/0.37	44.79/0.06	45.21/0.09
J0017.6-0512	0.227	IF	41.46/0.02	44.40/0.04	43.78/0.11	44.48/0.05	0.49/0.01	1.19/0.05	-0.11/0.01	14.48/0.13	44.53/0.15	45.02/0.21
J0018.4+2947	0.100	HB	40.00/0.01		43.54/0.07	42.84/0.13			-0.06/0.01	16.60/0.45	43.44/0.12	43.96/0.16
J0018.9-8152		HB			45.37/0.09	45.15/0.05			-0.05/0.01	17.16/0.45	45.33/0.07	45.90/0.07
J0019.1-5645		LJ				44.88/0.09			-0.13/0.01	13.35/0.10	44.34/0.06	44.41/0.10
J0019.4+2021		LB	43.04/0.01	44.42/0.04		44.91/0.10	0.75/0.01		-0.17/0.01	12.84/0.09	45.19/0.06	45.50/0.10
J0021.6-2553		LB	41.88/0.01	45.06/0.14		45.14/0.05	0.43/0.03		-0.17/0.02	13.77/0.17	45.43/0.08	45.67/0.12
J0021.6-6835		IU			44.82/0.08	44.27/0.12			-0.09/0.01	14.00/0.18	45.47/0.04	45.92/0.05
J0022.1-1855		IB	41.39/0.02	45.40/0.02	44.36/0.11	45.13/0.05	0.24/0.01	1.38/0.05	-0.13/0.01	14.69/0.12	45.46/0.03	45.76/0.05
J0022.1-5141		HB			45.51/0.07	45.11/0.05			-0.09/0.00	15.86/0.15	45.39/0.03	46.07/0.05
J0022.5+0608		LB	42.57/0.01	44.64/0.04		45.68/0.03	0.63/0.01		-0.12/0.01	13.58/0.12	45.30/0.06	45.40/0.09
...	...	...	...	...	...	...	...	...	...	...	...	...
...	...	...	...	...	...	...	...	...	...	...	...	...

Monochromatic Luminosity

Effective spectral index

Fitting Results P1,P2,P3

广州大学
Guangzhou University

Redshifts are available for 999 Fermi blazars, for which we made a distribution for the logarithm of their peak frequency at the comoving frame.

Bayesian information criterion for model selection, we used 9 components to fit the distribution, but 3 components are enough.

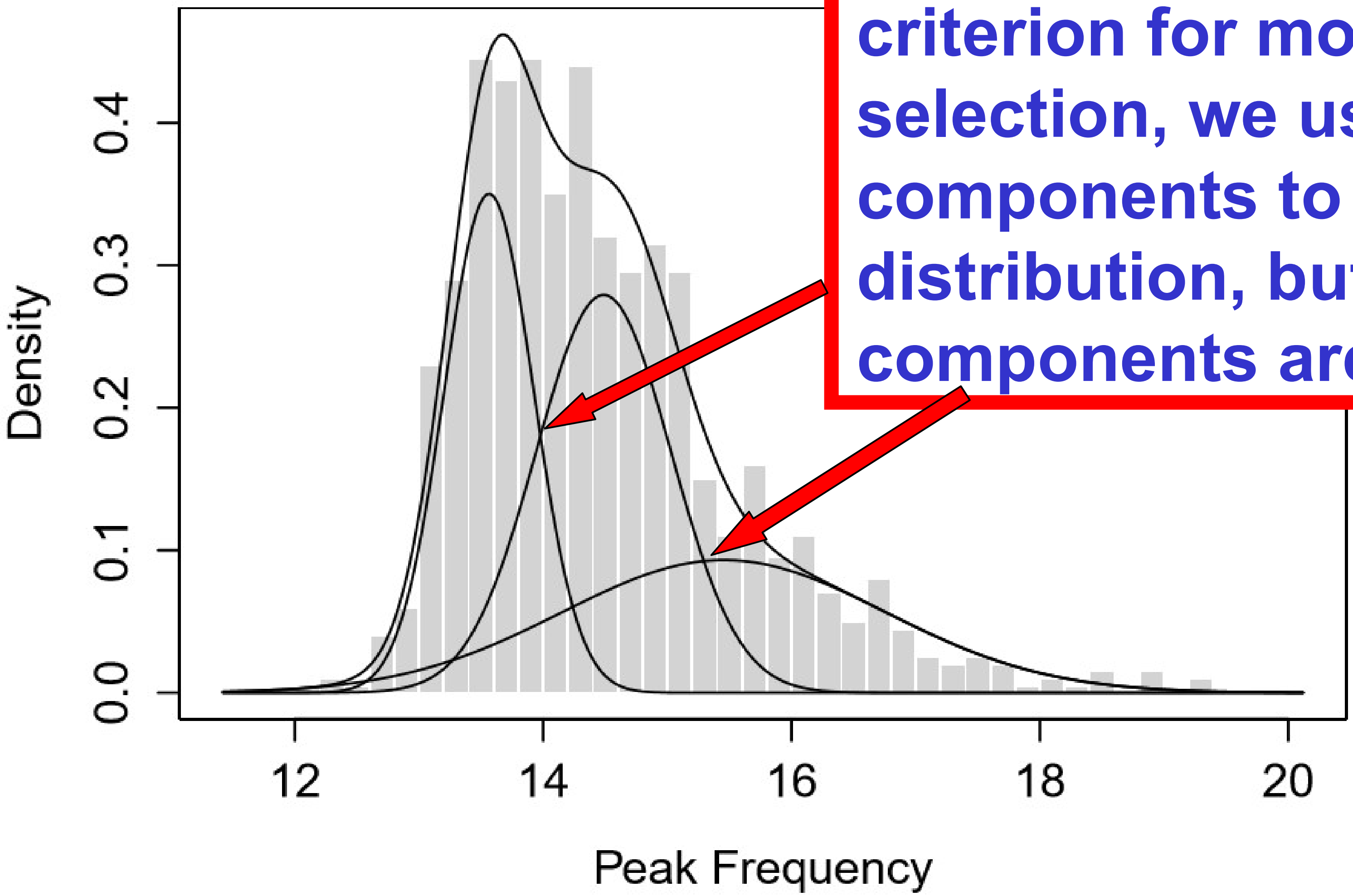

2.2 Classifications of Fermi Blazars

$$\log \nu_{\rm p}({\rm Hz}) \leq 14.0 \text{ for LSPs,}$$

$$14.0 < \log \nu_{\rm p}({\rm Hz}) \leq 15.3 \text{ for ISPs,}$$

$$\log \nu_{\rm p}({\rm Hz}) > 15.3 \text{ for HSPs.}$$

There is no ultra-high synchrotron peak sources-UHSPs as claimed by Ghisellini et al. (1999)

Boundaries for Classifications

LBL Log ν (Hz)	IBL Log ν (Hz)	HBL Log ν (Hz)	Ref
< 15		> 15	Padovani & Giommi, 1996
< 14.5	14.5 ~ 16.5	> 16.5	Nieppola et al. 2006
<14	14 ~ 15	> 15	Abdo et al. 2010
<14.0	14.0 ~ 15.3	>15.3	This work

Our results are similar to those by Abdo et al. 2010

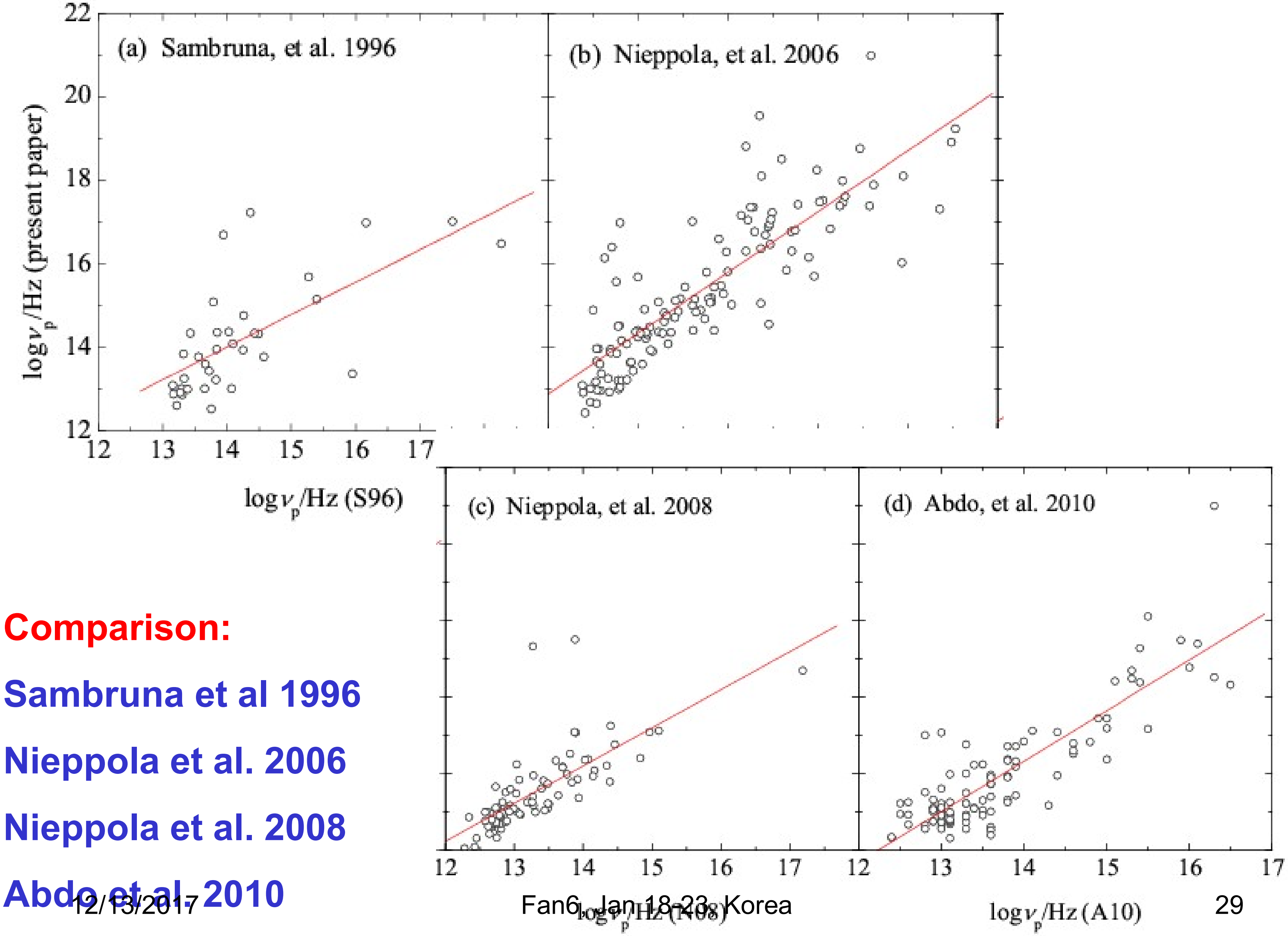

Comparison:

Sambruna et al 1996

Nieppola et al. 2006

Nieppola et al. 2008

Abdo et al. 2010

2.4 Luminosity Correlations

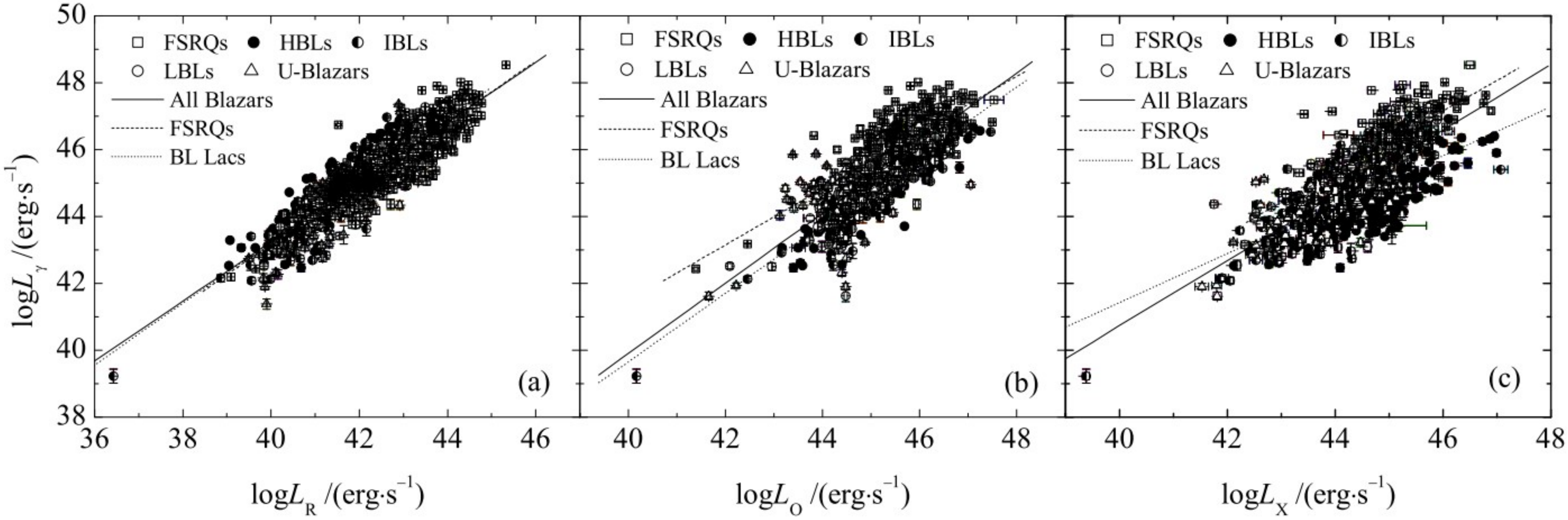

γ - radio **γ - optical** **γ - X-ray**

2.4 Luminosity Correlations

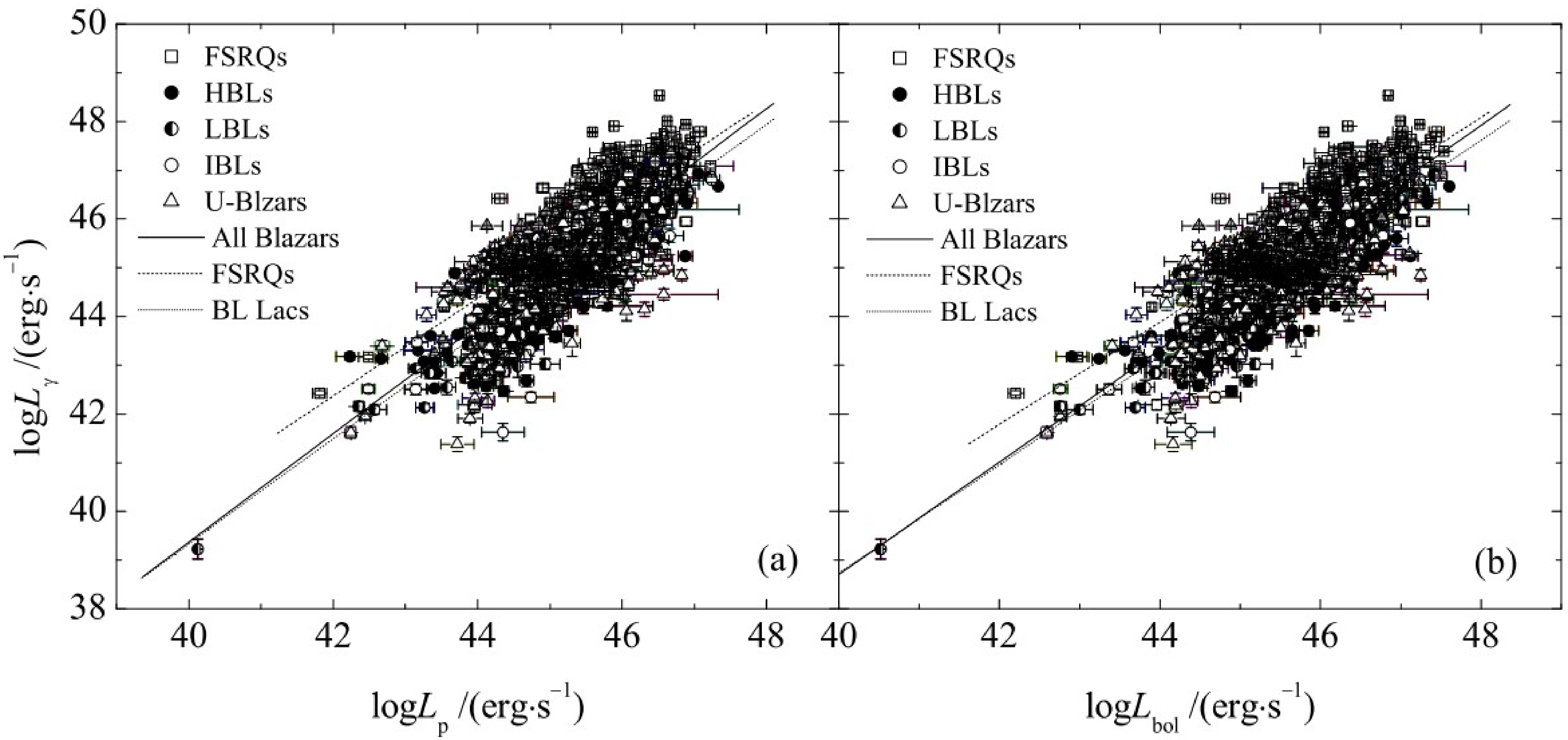

All the above correlations are significant

2.5 $logL\nu_p - log\nu_p$

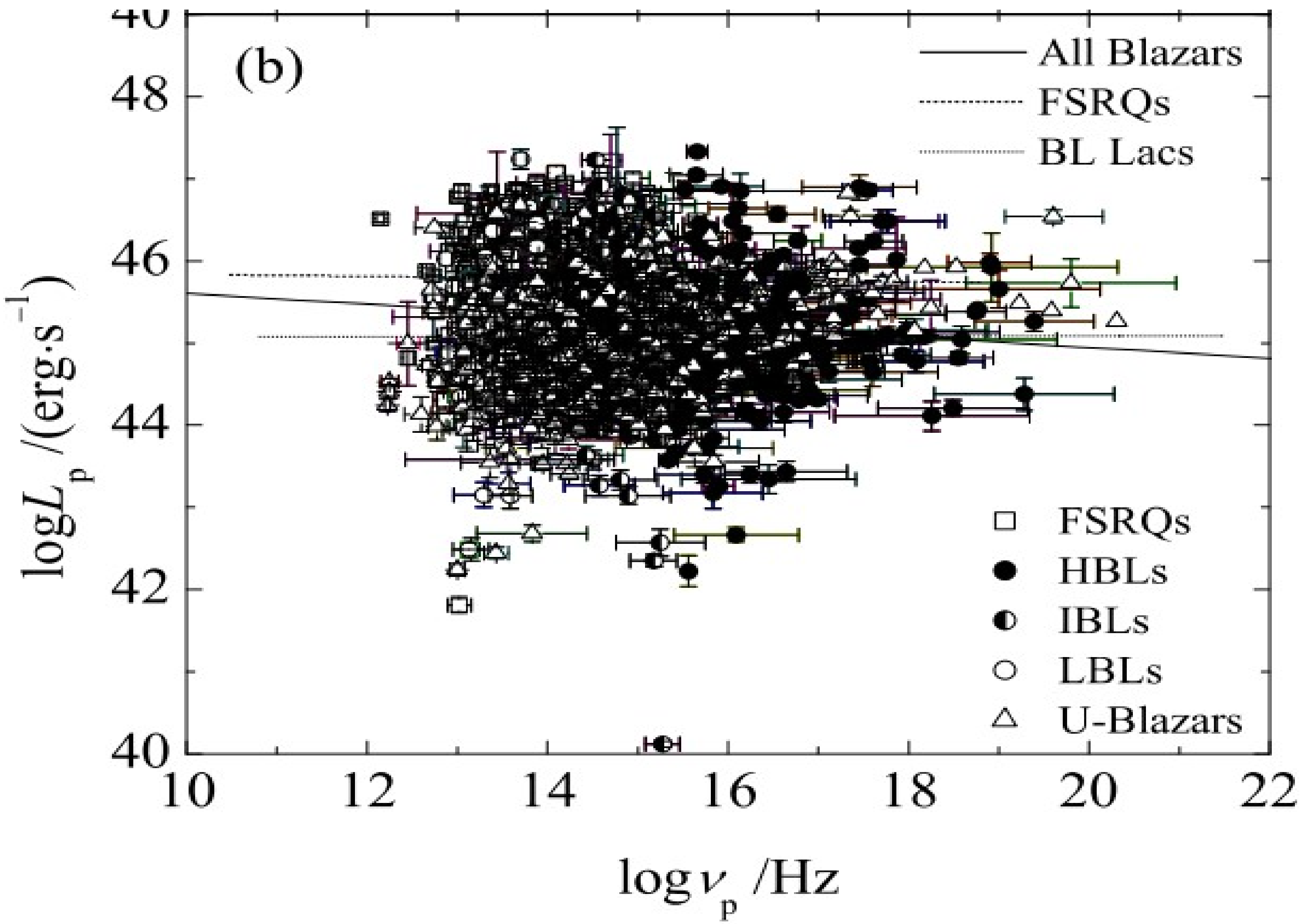

2.5 $logL_\gamma - log\nu_p$

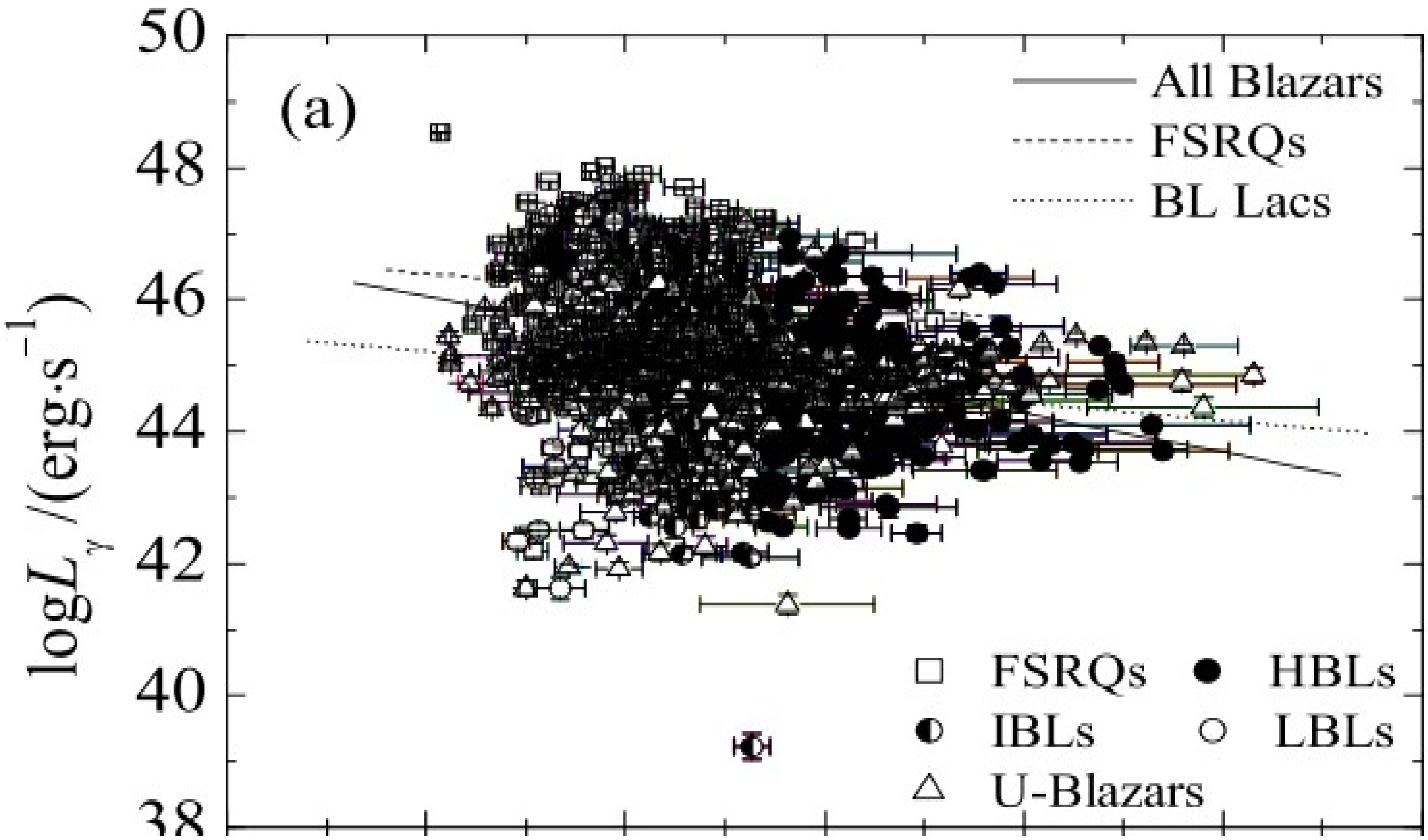

$log\nu_p$

2.5 P1 $- log\nu_p$

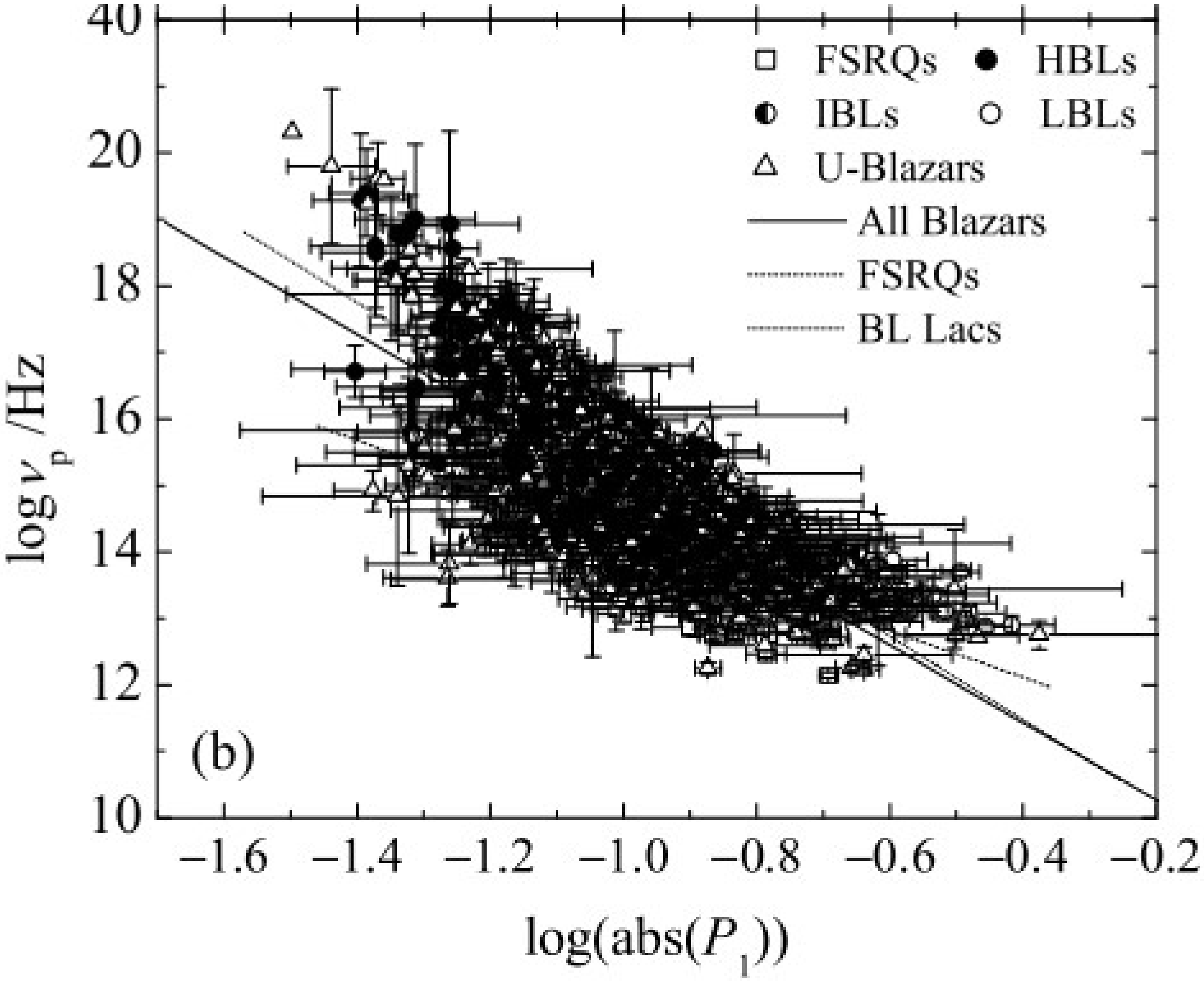
FSRQs
HBLs
IBLs
LBLs
U-Blazars
All Blazars
FSRQs
BL Lacs
(b)
$\log \nu_p$ /Hz
log(abs(P_1))
40
20
18
16
14
12
10
−1.6
−1.4
−1.2
−1.0
−0.8
−0.6
−0.4
−0.2

2.6 Empirical Function for Peak Frequency

$$\log \nu_{\rm p}^{\rm Eq.} = \begin{cases} 16 + 4.238X & X < 0 \\ 16 + 4.005Y & X > 0 \end{cases}$$

$$X = 1.0 - 1.262\alpha_{ro} - 0.623\alpha_{ox},$$

$$Y = 1.0 + 0.034\alpha_{ro} - 0.978\alpha_{ox}$$

2.6 Empirical Function for Peak Frequency

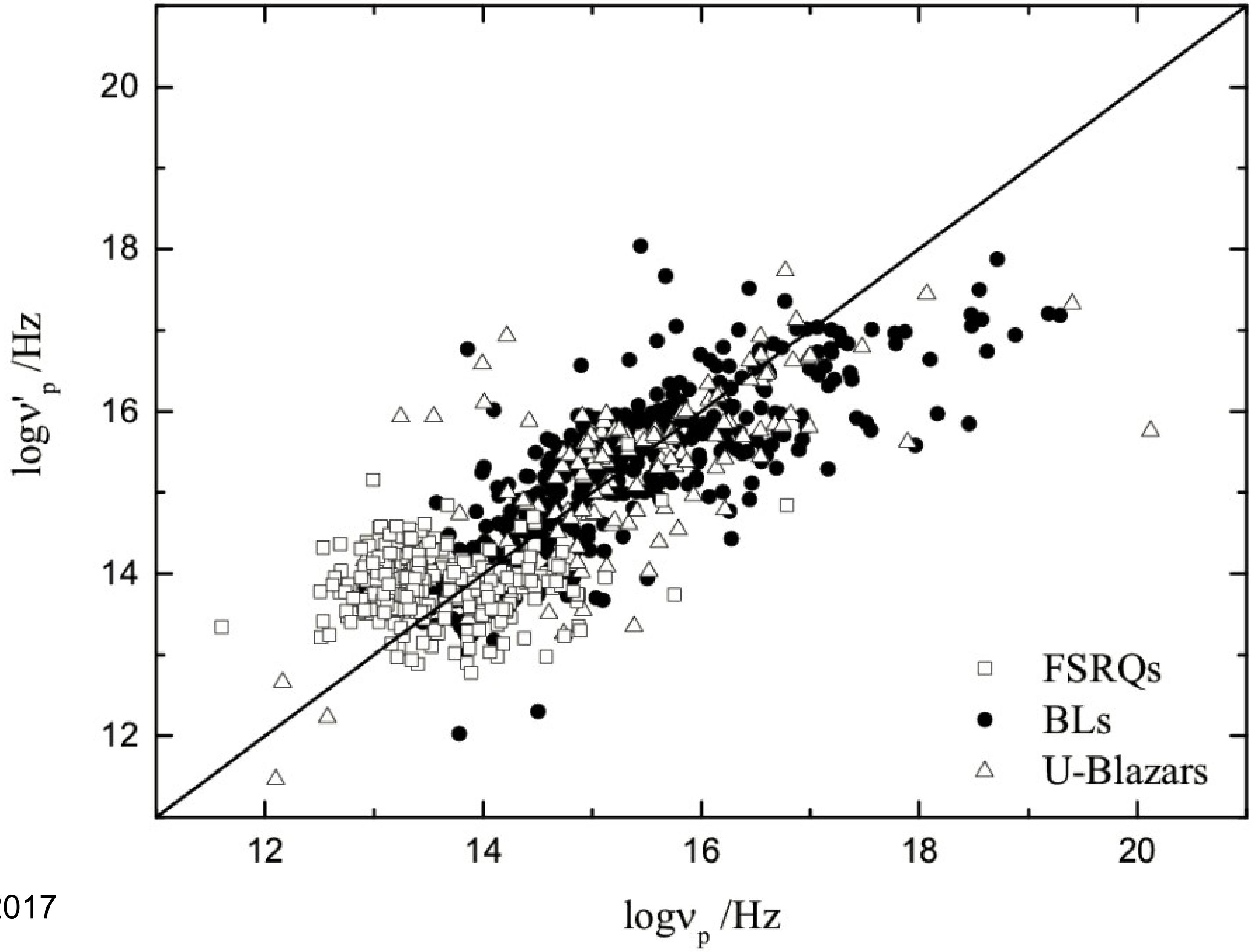

Outline

3. Beaming Effect in Fermi Blazars

3.1 Radio polarization
3.2 Radio and Gamma-Ray Correlation
3.3 etc ……

3.1 Radio Polarization in Fermi Sources

Hovatta et al. 2010, IJMPD

They found that the radio polarization in the FERMI detected era is higher for the investigated sources.

In factor, we obtained that the polarization is associated with the Doppler factor (Fan, Cheng, Zhang, 1997, A&A) .

3.1 Polarization & Beaming effect

Fan, Cheng, Zhang, 1997, A&A
Fan, 2002, PASJ

$$P_{ob} = \frac{(1+f)\delta_o^p}{1+f\delta_o^p} P_{in}$$

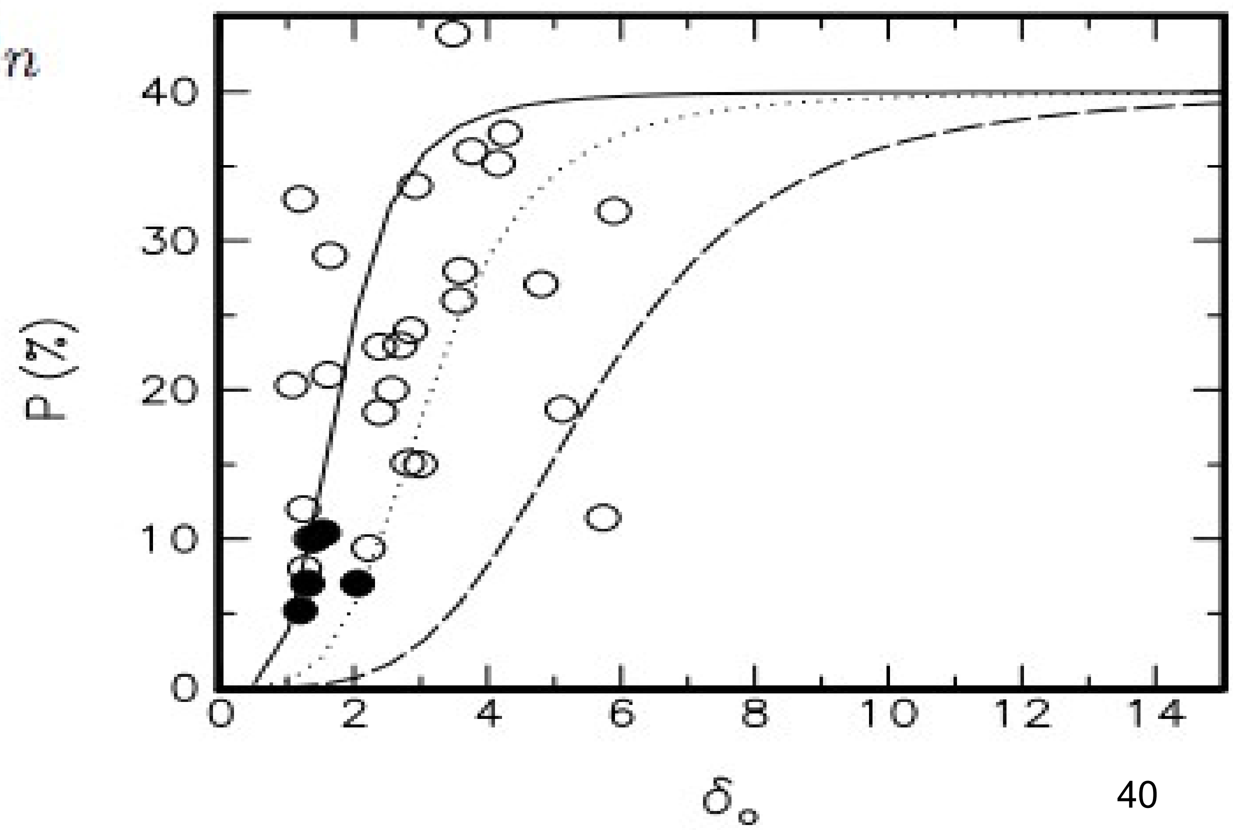

广州大学 Guangzhou University

3.2. Radio and Gamma-ray Correlation

Gamma-Ray VS. 325 MHz

Massaro, et al. 2014, IAUS304

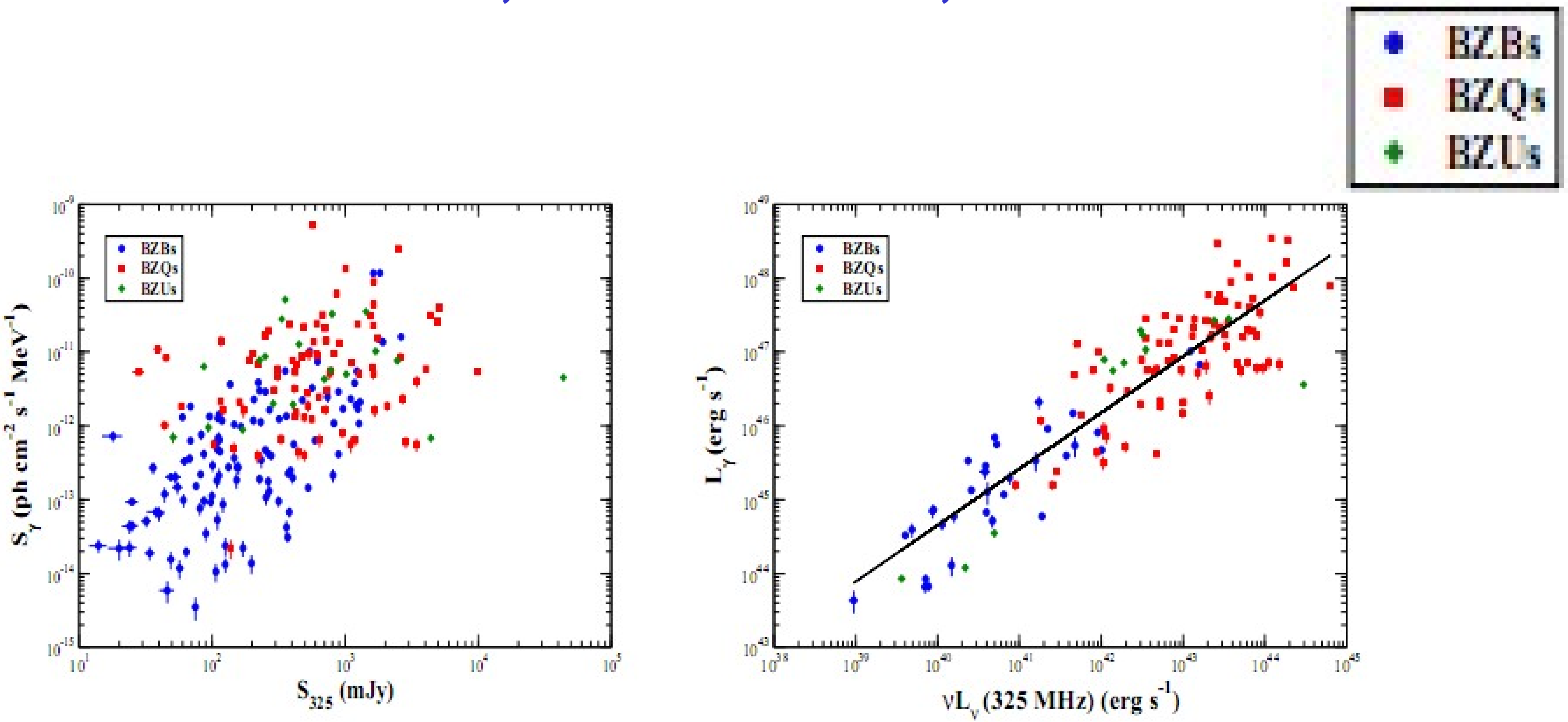

Radio-faint BL Lac objects and their impact on the radio/gamma-ray connection

Giroletti, M, Pavlidou, V., Reimer, A. et al. 2012, AdSpR, 49

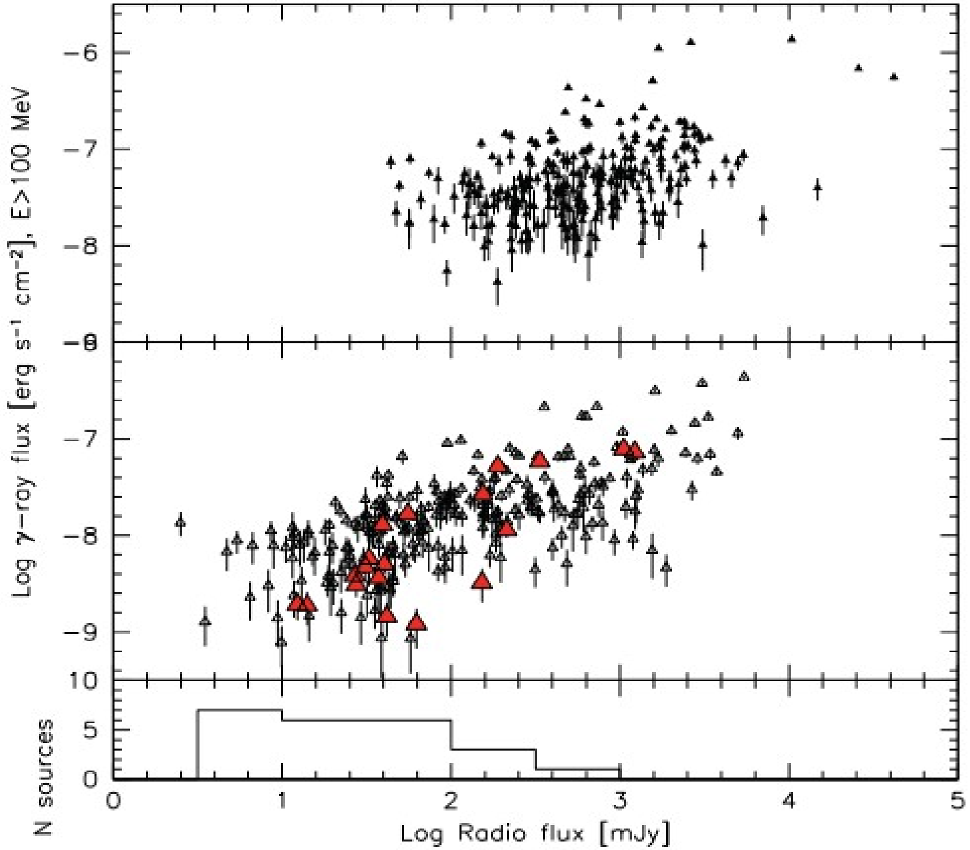

FSRQs

BL Lacs

8.4GHz

Fig. 3. Top and middle panels: mean 1-yr $E > 100$ MeV gamma-ray flux vs. radio flux density at 8.4 GHz for 1FGL sources; top: FSRQs; middle: BL Lacs (the big red triangles show the BL Lacs from the sample presented in this work). The bottom panel shows the radio flux density

Gamma-Ray VS. 1.4 GHz

Fan， J.H.; Yang，J.H.; Liu， Y. , et al. 2016, ApJS

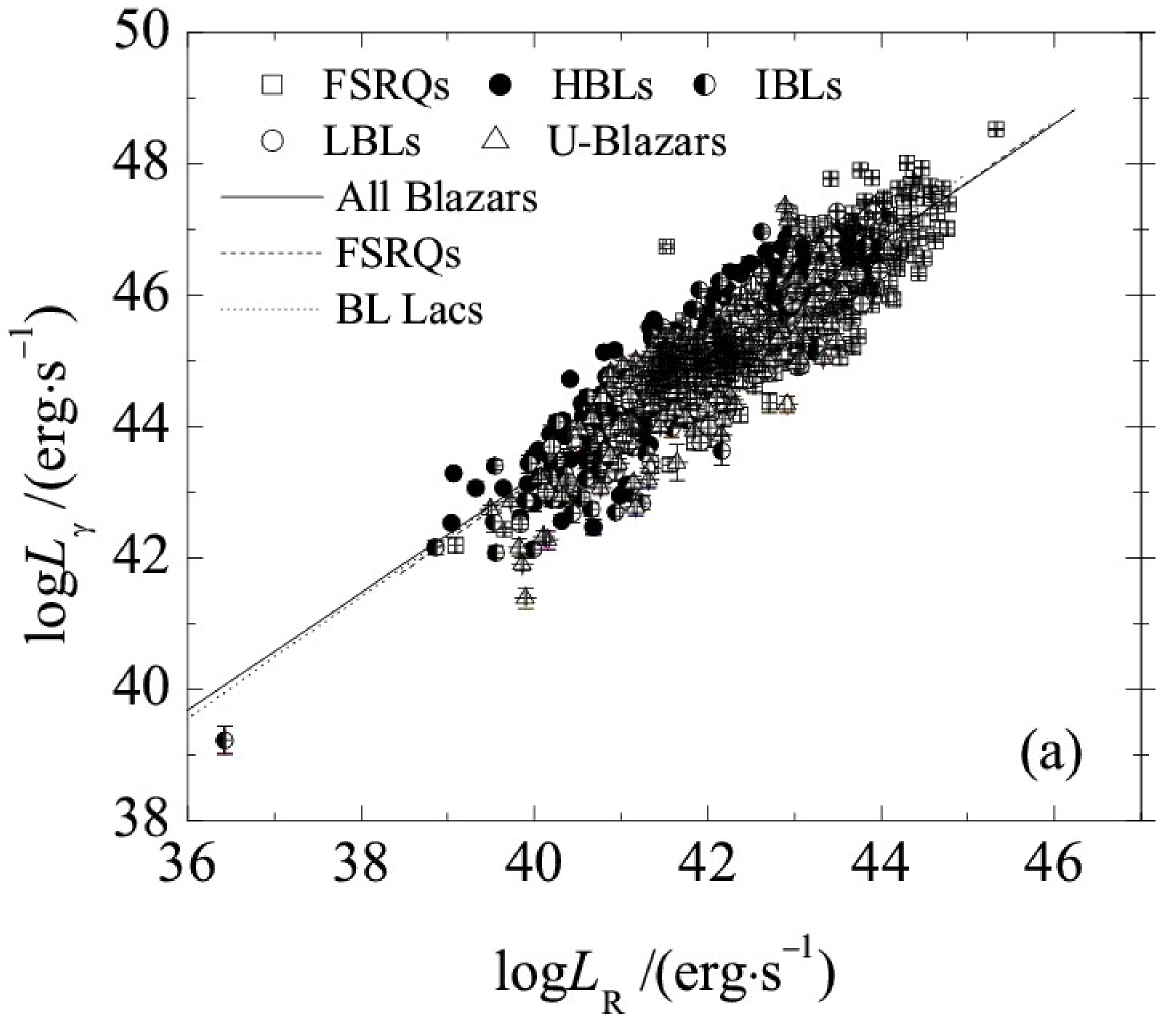

Gamma-Radio From EGRET

Fan et al. 1998, A&A

EGRET

230GHz

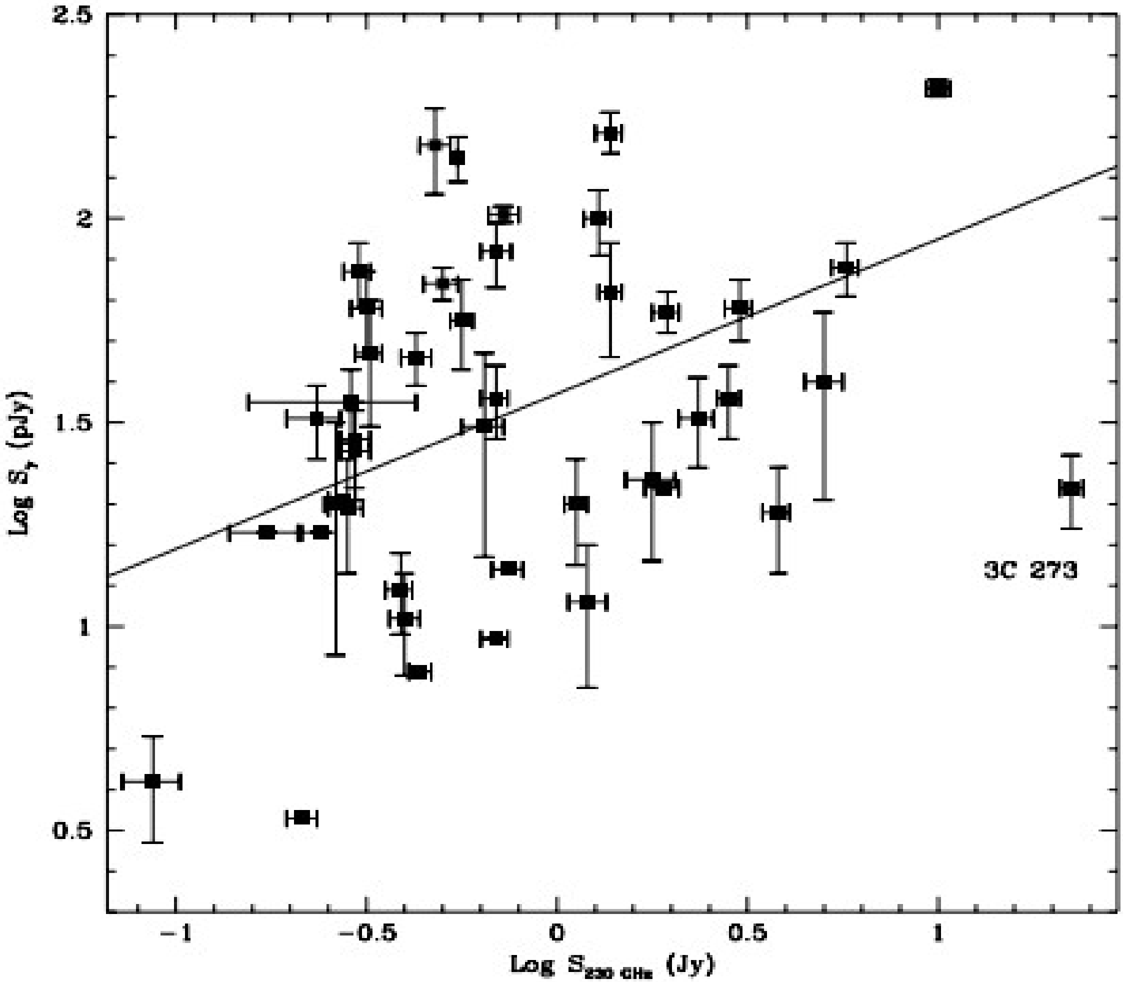

Fig. 2. The diagram of γ-ray flux density in pJy against the radio flux density in Jy at 230 GHz, the solid line shows the best fit with $3C273$

3.1 Radio polarization

3.2 Radio and Gamma-Ray Correlation

3.3 etc ……

Gamma-ray emissions may be strongly beamed.

3.3 Luminosity vs. peak frequency

Fan, J.H. et al. 2017, ApJL, 835, 38
Fermi Blazars with Doppler Factors
"Blazar sequence" is a selection effect

In this work, we got a sample of Fermi Blazars with available Doppler factors. Then we investigated the correlations between luminosity and Doppler factor. Correlations between monochromatic luminosities, and those between luminosity and peak frequency for the observed and the intrinsic (Beaming effect removed) data .

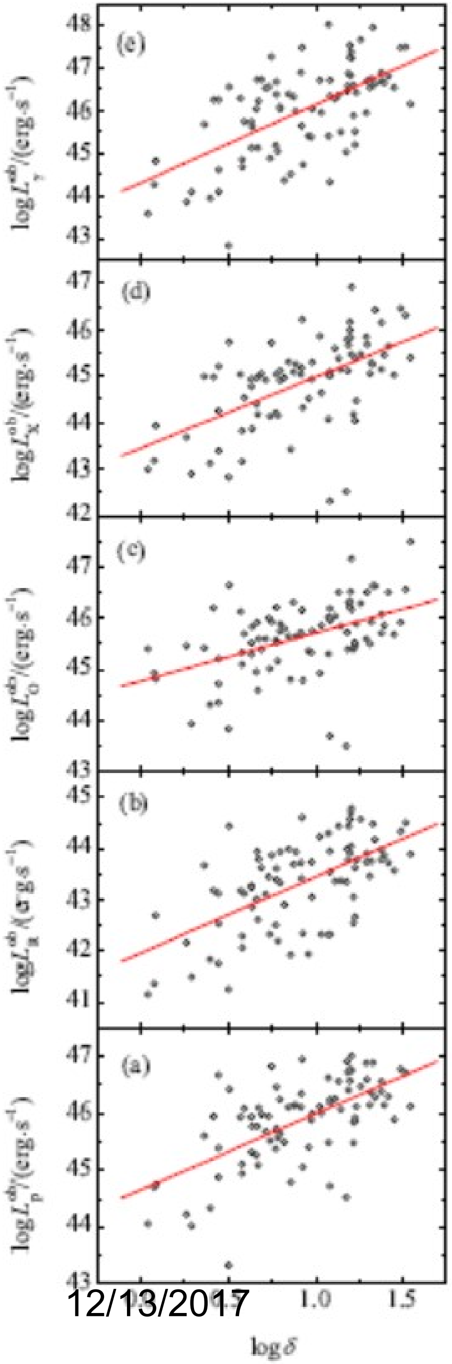

Fan, J.H. et al. 2017, ApJL, 835, 38
Fermi Blazars with Doppler Factors

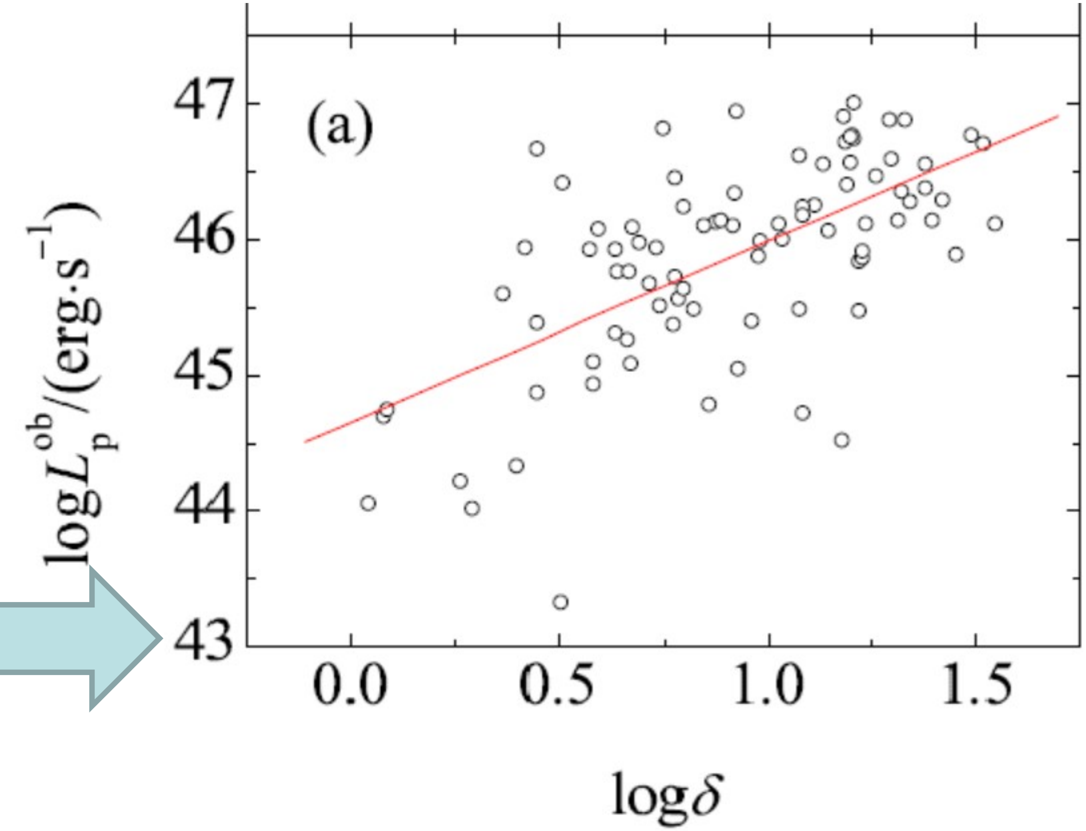

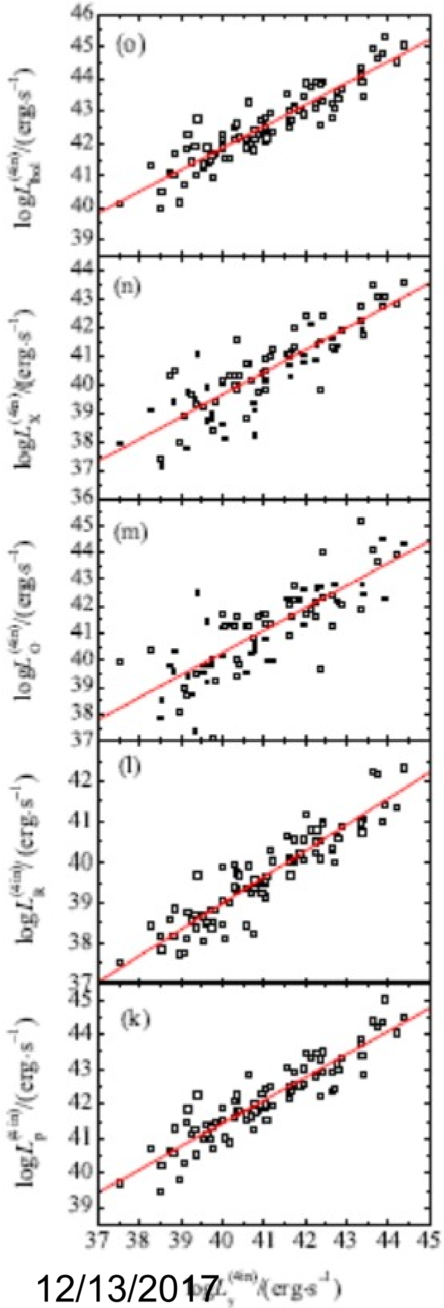

Top to the bottom is for bolometric, X-ray, optical, radio, and peak luminosity

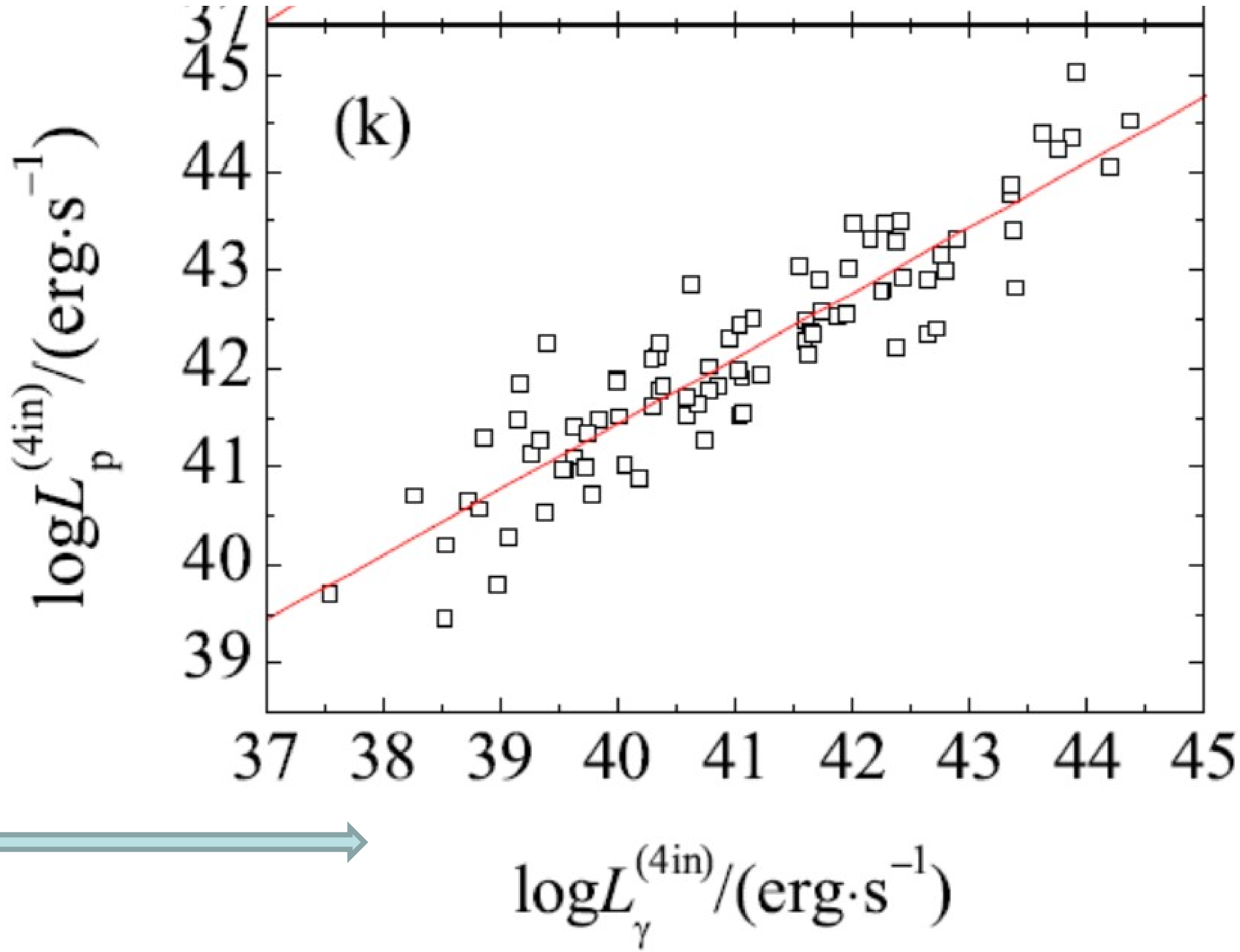

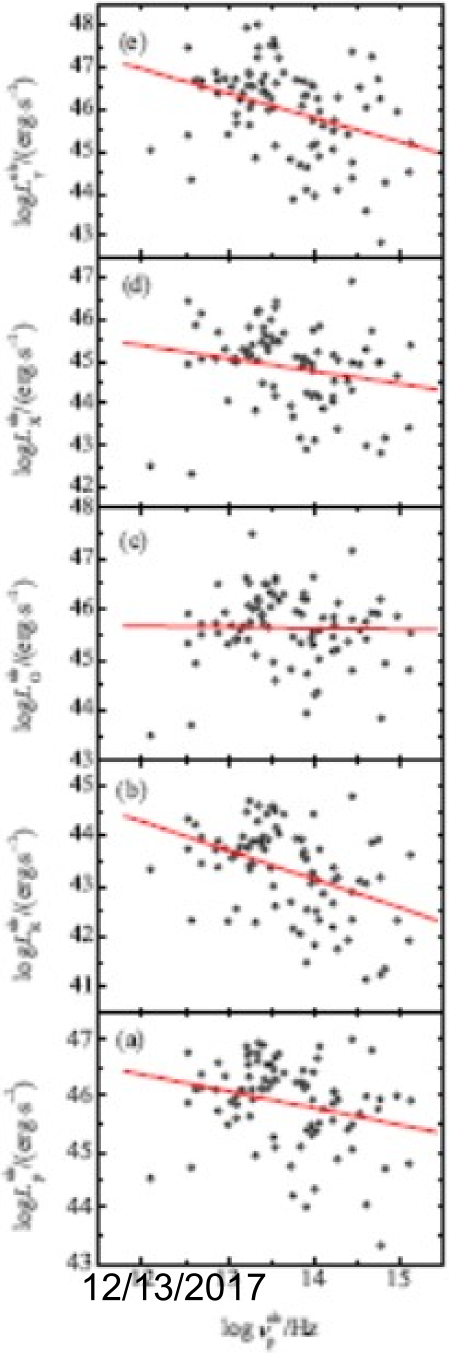

Top one to the bottom one is for γ -ray, X-ray, optical, radio, and peak luminosities.

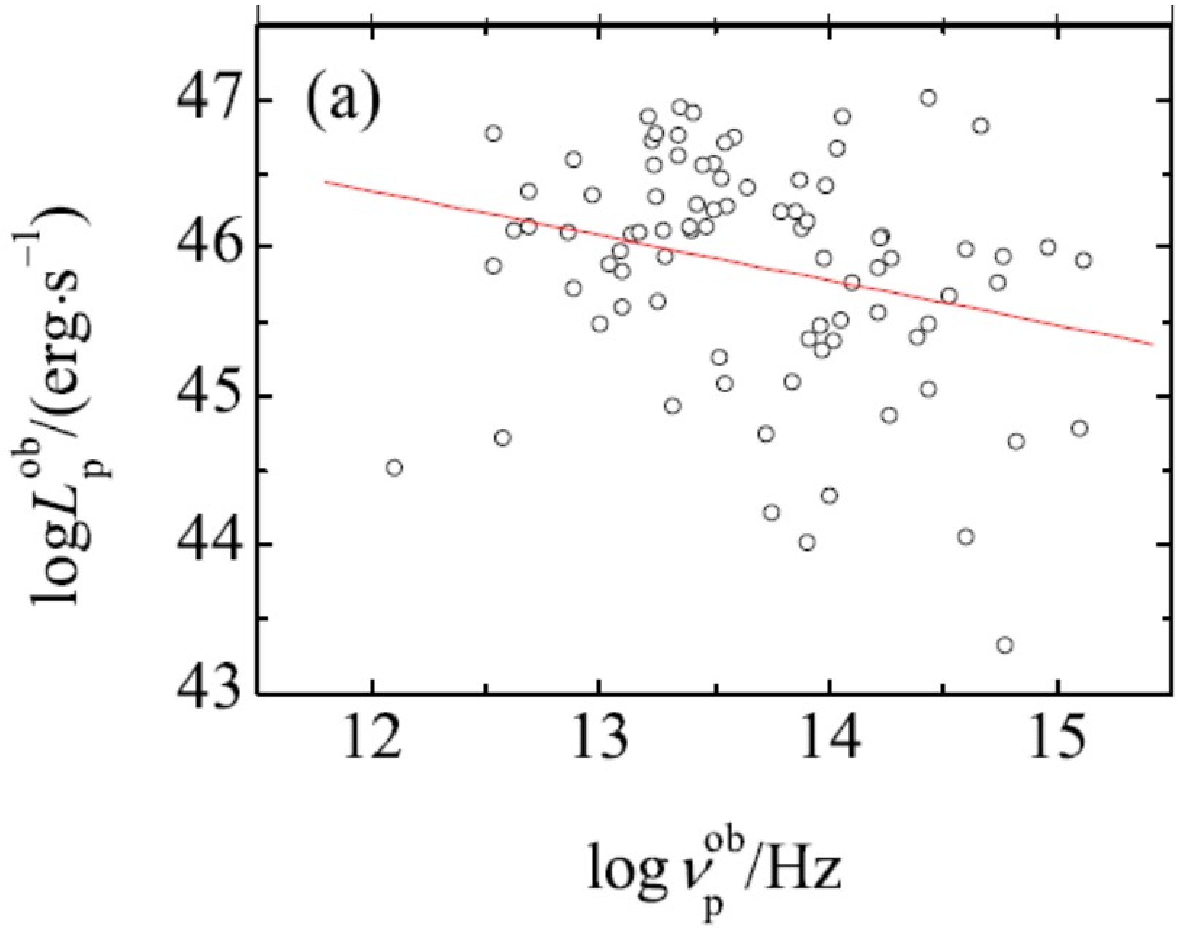

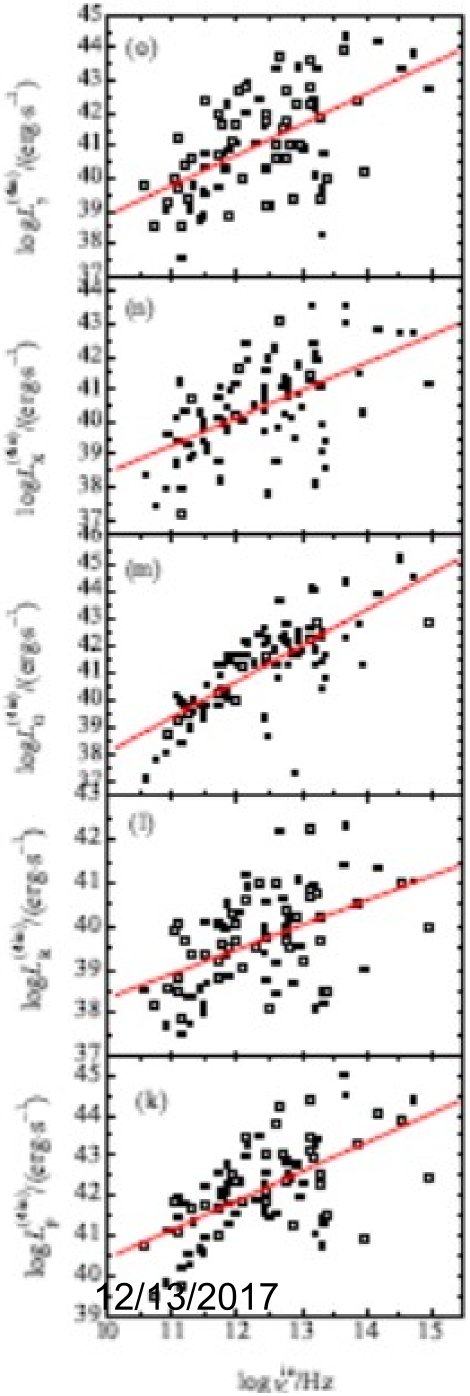

Top one to the bottom one is for γ -ray, X-ray, optical, radio, and peak luminosities.

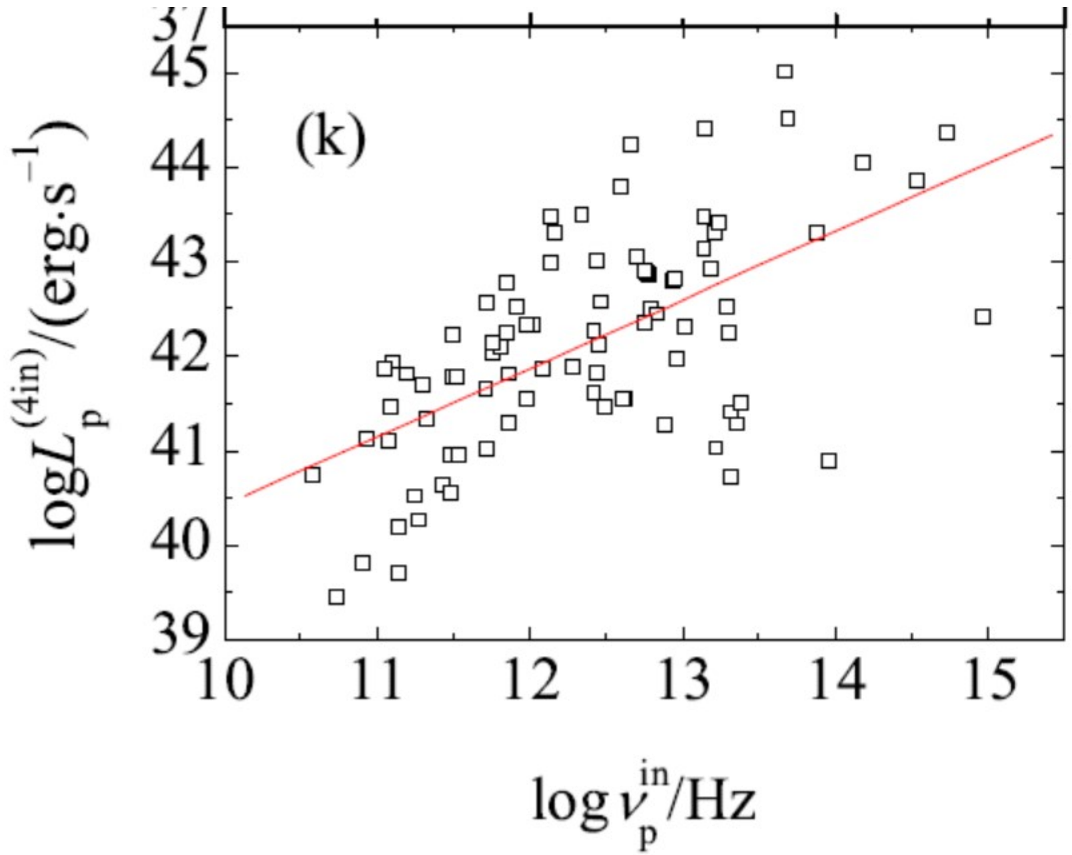

$y \sim x$	$a \sim \Delta a$	$b \sim \Delta b$	N	r	p
$\log L_p^{ob} \sim log\delta$	44.656 ± 0.178	1.330 ± 0.181	86	0.625	1.22×10^{-10}
$\log L_R^{ob} \sim log\delta$	41.963 ± 0.209	1.484 ± 0.212	86	0.606	6.14×10^{-10}
$\log L_o^{ob} \sim log\delta$	44.775 ± 0.190	0.935 ± 0.193	86	0.468	5.62×10^{-6}
$\log L_X^{ob} \sim log\delta$	43.456 ± 0.239	1.521 ± 0.242	82	0.575	1.60×10^{-8}
$\log L_\gamma^{ob} \sim log\delta$	44.304 ± 0.252	1.832 ± 0.257	86	0.614	3.15×10^{-10}
$\log L_p^{3in} \sim logL_\gamma^{3in}$	18.472 ± 1.603	0.586 ± 0.038	86	0.858	4.49×10^{-26}
$\log L_R^{3in} \sim logL_\gamma^{3in}$	16.675 ± 1.561	0.570 ± 0.037	86	0.858	4.86×10^{-26}
$\log L_O^{3in} \sim logL_\gamma^{3in}$	11.650 ± 3.399	0.725 ± 0.081	86	0.699	7.36×10^{-14}
$\log L_X^{3in} \sim logL_\gamma^{3in}$	11.591 ± 2.752	0.710 ± 0.066	82	0.771	2.43×10^{-17}
$\log L_{bol}^{3in} \sim logL_\gamma^{3in}$	18.698 ± 1.572	0.590 ± 0.037	86	0.864	8.03×10^{-27}
$\log L_p^{4in} \sim logL_\gamma^{4in}$	14.822 ± 1.314	0.665 ± 0.032	86	0.915	6.91×10^{-35}
$\log L_R^{4in} \sim logL_\gamma^{4in}$	13.049 ± 1.261	0.648 ± 0.031	86	0.917	2.35×10^{-35}
$\log L_O^{4in} \sim logL_\gamma^{4in}$	7.134 ± 2.806	0.829 ± 0.068	86	0.798	3.68×10^{-20}
$\log L_X^{4in} \sim logL_\gamma^{4in}$	8.452 ± 2.242	0.780 ± 0.055	82	0.847	1.04×10^{-23}
$\log L_{bol}^{4in} \sim logL_\gamma^{4in}$	15.052 ± 1.293	0.670 ± 0.031	86	0.918	1.39×10^{-35}
$\log L_p^{ob} \sim log\nu_p^{ob}$	49.986 ± 1.678	-0.300 ± 0.122	86	-0.259	1.6%
$\log L_R^{ob} \sim log\nu_p^{ob}$	51.138 ± 1.808	-0.571 ± 0.132	86	-0.427	4.15×10^{-5}
$\log L_O^{ob} \sim log\nu_p^{ob}$	45.921 ± 1.633	-0.021 ± 0.119	86	-0.019	86%
$\log L_X^{ob} \sim log\nu_p^{ob}$	49.027 ± 2.197	-0.304 ± 0.160	82	-0.208	6.1%
$\log L_\gamma^{ob} \sim log\nu_p^{ob}$	53.918 ± 2.276	-0.580 ± 0.166	86	-0.356	7.73×10^{-4}
$\log L_p^{3in} \sim log\nu_p^{3in}$	37.472 ± 1.081	0.451 ± 0.087	86	0.492	1.53×10^{-6}
$\log L_R^{3in} \sim log\nu_p^{3in}$	36.971 ± 1.141	0.292 ± 0.092	86	0.327	2.13×10^{-3}
$\log L_O^{3in} \sim log\nu_p^{3in}$	29.299 ± 1.268	1.033 ± 0.102	86	0.740	3.71×10^{-16}
$\log L_X^{3in} \sim log\nu_p^{3in}$	34.302 ± 1.496	0.571 ± 0.121	82	0.468	9.31×10^{-6}
$\log L_\gamma^{3in} \sim log\nu_p^{3in}$	33.734 ± 1.581	0.666 ± 0.128	86	0.495	1.26×10^{-6}
$\log L_p^{4in} \sim log\nu_p^{4in}$	33.228 ± 1.285	0.720 ± 0.104	86	0.604	7.26×10^{-10}
$\log L_R^{4in} \sim log\nu_p^{4in}$	32.727 ± 1.372	0.561 ± 0.111	86	0.484	2.33×10^{-6}
$\log L_O^{4in} \sim log\nu_p^{4in}$	25.056 ± 1.485	1.302 ± 0.120	86	0.765	1.07×10^{-17}
$\log L_X^{4in} \sim log\nu_p^{4in}$	30.024 ± 1.704	0.842 ± 0.137	82	0.566	3.08×10^{-8}
$\log L_\gamma^{4in} \sim log\nu_p^{4in}$	29.490 ± 1.822	0.935 ± 0.147	86	0.570	9.94×10^{-10}

广州大学 Guangzhou University

4. Discussions and Summary

1. Fitted SEDs for 1425 Fermi blazars, setting boundaries for LSPs, ISPs, and HSPs, compared our results with others

$$\log \nu_{\rm p}({\rm Hz}) \leq 14.0 \text{ for LSPs,}$$

$$14.0 < \log \nu_{\rm p}({\rm Hz}) \leq 15.3 \text{ for ISPs,}$$

$$\log \nu_{\rm p}({\rm Hz}) > 15.3 \text{ for HSPs.}$$

No UHSPs

2. An empirical relation between the peak frequency and effective spectral index

$$\log\nu_{\rm p}^{\rm Eq.} = \begin{cases} 16 + 4.238X & X < 0 \\ 16 + 4.005Y & X > 0 \end{cases},$$

where $X = 1.0 - 1.262\alpha_{ro} - 0.623\alpha_{ox}$, and $Y = 1.0 + 0.034\alpha_{ro} - 0.978\alpha_{ox}$.

3. Correlations are investigated. Gamma-rays are more closely correlated with radio emissions; Gamma-ray sources are radio loud
4. Gamma-ray emissions are strongly beamed
5. Blazar-sequence is a selected result

Thank you for your attention!

Thank you for your attention!

祝各位健康、平安、进步！